**Atmospheric
Chemistry
and Physics
Discussions**

Observations of volatile organic compounds during ARCTAS – Part 1: Biomass burning emissions and plume enhancements

R. S. Hornbrook[1], D. R. Blake[2], G. S. Diskin[3], H. E. Fuelberg[4], S. Meinardi[2], T. Mikoviny[5], G. W. Sachse[3], S. A. Vay[3], A. J. Weinheimer[1], C. Wiedinmyer[1], A. Wisthaler[5], A. Hills[1], D. D. Riemer[6], and E. C. Apel[1]

[1]Atmospheric Chemistry Division, National Center for Atmospheric Research, Boulder, CO, USA
[2]Department of Chemistry, University of California Irvine, Irvine, CA, USA
[3]NASA Langley Research Center, Hampton, VA, USA
[4]Department of Meteorology, Florida State University, Tallahassee, FL, USA
[5]Institut für Ionenphysik & Angewandte Physik, University of Innsbruck, Innsbruck, Austria
[6]Rosenstiel School of Marine and Atmospheric Science, University of Miami, Miami, FL, USA

ACPD

11, 14127–14182, 2011

**ARCTAS VOCs:
biomass burning
enhancements**

R. S. Hornbrook et al.

Title Page

Abstract	Introduction
Conclusions	References
Tables	Figures

◀◀   ▶▶

◀   ▶

Back   Close

Full Screen / Esc

Printer-friendly Version

Interactive Discussion

ARCTAS VOCs: biomass burning enhancements

R. S. Hornbrook et al.

Title Page

Abstract	Introduction
Conclusions	References
Tables	Figures

|◄ ►|

◄ ►

| Back | Close |

Full Screen / Esc

Printer-friendly Version

Interactive Discussion

Abstract

Mixing ratios of a large number of volatile organic compounds (VOCs) were observed by the Trace Organic Gas Analyzer (TOGA) on board the NASA DC-8 as part of the Arctic Research of the Composition of the Troposphere from Aircraft and Satellites (ARCTAS) field campaign. Many of these VOCs were observed concurrently by one or both of two other VOC measurement techniques on board the DC-8: proton-transfer-reaction mass spectrometry (PTR-MS) and whole air canister sampling (WAS). A comparison of these measurements to the data from TOGA indicates good agreement for the majority of co-measured VOCs. The ARCTAS study, which included both spring and summer deployments, provided opportunities to sample a large number of biomass burning (BB) plumes with origins in Asia, California and Central Canada, ranging from very recent emissions to plumes aged one week or more. For this analysis, identified BB plumes were grouped by flight, source region and, in some cases, time of day, generating 40 individual plume groups, each consisting of one or more BB plume interceptions. Normalized excess mixing ratios (EMRs) to CO were determined for each of the 40 plume groups for up to 19 different VOCs or VOC groups, many of which show significant variability, even within relatively fresh plumes. This variability demonstrates the importance of assessing BB plumes both regionally and temporally, as emissions can vary from region to region, and even within a fire over time. Comparisons with literature confirm that variability of EMRs to CO over an order of magnitude for many VOCs is consistent with previous observations. However, this variability is often diluted in the literature when individual observations are averaged to generate an overall regional EMR from a particular study. Previous studies give the impression that emission ratios are generally consistent within a given region, and this is not necessarily the case, as our results show. For some VOCs, earlier assumptions may lead to significant under-prediction of emissions in fire emissions inventories. Notably, though variable between plumes, observed EMRs of individual light alkanes are highly correlated within BB emissions. Using the NCAR master mechanism chemical box model

Title Page

Abstract	Introduction
Conclusions	References
Tables	Figures

◄◄ ►►

◄ ►

Back Close

Full Screen / Esc

Printer-friendly Version

Interactive Discussion

initialized with concentrations based on two observed scenarios, i.e., fresh Canadian BB and fresh Californian BB, both plumes are expected to experience primarily decreases in oxygenated VOCs during the first 2.5 days, such that any production in the plumes of these compounds is less than the chemical loss. Comparisons of the modeled EMRs to the observed EMRs from BB plumes estimated to be three days in age or less indicate overall good agreement and, for most compounds, no significant difference between BB plumes in these two regions.

1 Introduction

Biomass burning (BB) is a significant source of gases and particles to the regional and global atmosphere, playing an important role in the chemistry and radiative transfer of the atmosphere (Levine, 2000). Although the majority of BB occurs in the tropics, fires in extratropical regions can impact both local and regional air quality (Colarco et al., 2004; Morris et al., 2006), and contribute to climate change and the chemistry of polar atmospheres (Damoah et al., 2004; Vivchar et al., 2010; Tilmes et al., 2010). Due to convection and pyroconvection, BB plumes from boreal forests can inject trace gases and aerosols into the upper troposphere and lower stratosphere, where long-range transport can widely distribute the emissions (Fromm et al., 2000; Jost et al., 2004; Val Martin et al., 2010). Although there have been a number of laboratory studies of volatile organic compound (VOC) emissions (sometimes referred to as non-methane organic compound (NMOC) emissions) from BB (Christian et al., 2003, 2004; Yokelson et al., 2008) as well as both near-field (Friedli et al., 2001; Jost et al., 2003; Sinha et al., 2003, 2004; Christian et al., 2007; Yokelson et al., 2007a,b; 2009) and long-range transport studies of fire plumes (Holzinger et al., 2005; de Gouw et al., 2006; Duck et al., 2007; Yuan et al., 2010), emissions of trace VOCs from BB and the chemical evolution of these compounds within the plumes remain relatively uncertain (de Gouw et al., 2006; Monks et al., 2009). This is particularly true for emissions of oxygenated VOCs (OVOCs), as evidenced by the factor of 3.7 to 4.9 increase of NMOC emissions

in a recent fire emissions inventory over previous inventories to account for additional OVOCs, many not quantitatively identified by presently-available observation methods (Wiedinmyer et al., 2010).

The 2008 NASA Arctic Research of the Composition of the Troposphere from Aircraft and Satellites (ARCTAS) mission was part of the broader International Polar Year (IPY) collaborative effort POLARCAT (Polar Study using Aircraft, Remote Sensing, Surface Measurements and Models, of Climate, Chemistry, Aerosols, and Transport). ARC-TAS was a multi-platform field campaign involving airborne measurements from three NASA aircraft (DC-8, P-3B and B-200), a number of ground-based measurement sites and satellite observations. ARCTAS was held in coordination with other POLARCAT activities including the NOAA-led Aerosol, Radiation and Cloud Processes affecting Arctic Climate (ARCPAC) and the Greenland Aerosol and Chemistry Experiment (DLR-GRACE). An overview of the ARCTAS campaign has been published with a detailed description of all the measurement platforms and supporting investigations used during the campaign (Jacob et al., 2009). As well, an overview of the meteorology during ARCTAS and modeled back trajectories is available (Fuelberg et al., 2010).

The presented work in this paper and a following paper (Part 2) (Hornbrook et al., 2011) focus on measurements made on board the NASA DC-8 during ARCTAS. The DC-8 was involved in the three major components of the ARCTAS campaign: (a) ARCTAS-A, based in Fairbanks, Alaska with research flights in the Arctic regions of Canada, Alaska and Greenland between 1–19 April 2008, (b) ARCTAS-CARB, based in Palmdale, California, in co-operation with the California Air Resources Board with flights over California between 18–26 June 2008, and (c) ARCTAS-B, based in Alberta, Canada with flights over Central Canada and the Arctic regions of Canada and Greenland between 26 June–13 July 2008. In total, there were 9 flights during the spring and 13 flights during the summer.

Objectives for the three ARCTAS components were specific to each region of study, but sometimes overlapped, including long-range transport of pollution from mid-latitudes to the Arctic, ozone budgets, chemical processes, and aerosol radiative

ARCTAS VOCs: biomass burning enhancements

R. S. Hornbrook et al.

forcing. In both the spring and summer of 2008, there were a significant number of large scale BB events in the Northern Hemisphere, particularly in Siberia in April, and in California and Saskatchewan in late June and July, and thus all three ARCTAS components provided opportunities to study and characterize BB plumes. These plumes originated from a variety of source regions and ranged from fresh emissions to long-range transported plumes aged for up to a week or more. With several instruments that measured mixing ratios of many VOCs on board the DC-8, along with a suite of other trace gas measurements, this provided a valuable data set for quantifying the evolution of VOCs in BB plumes.

In this paper (part 1), we present an overview of the VOC observations, including a comparison of the observations from the different VOC measurement techniques used on board the DC-8 during ARCTAS. Flight time intervals when the DC-8 sampled BB plumes were identified using known fire tracers, and aircraft coordinates, back trajectories, and MODIS fire counts were used to determine the origin of each plume. These identified plumes were grouped by flight, source region and time-of-day into 40 BB plume groups for analysis. The relative enhancements of individual VOCs to longer-lived fire tracer species were determined for each group, analyzed with regards to BB plume age, and compared with previously-measured VOC enhancement ratios.

In part 2 (Hornbrook et al., 2011), we contrast BB emissions from different source regions from ARCTAS with urban emissions and anthropogenic point sources also sampled during the study. From observations of C_2–C_5 alkanes and C_6–C_8 aromatic hydrocarbons, we show that significant differences exist between the ratios of NMHC (non-methane hydrocarbons) in fire emissions and from anthropogenic activities. As well, we show that ratios of alkane isomers with nearly identical OH-removal rates (i.e.: isobutane/butane) can vary significantly between anthropogenic and primary fossil fuel point sources. We investigate the impact of these differences on emission inventories and regional and global VOC modeling.

2 Experimental technique

2.1 Aircraft measurements

The Trace Organic Gas Analyzer (TOGA) uses fast online gas chromatography coupled with mass spectrometry (GS-MS), analyzing a 40-s integrated sample once every two minutes, and was used to measure up to 28 different VOCs during ARCTAS. Major instrument components of the TOGA include the heated electropolished stainless steel (SS) inlet, cryogenic preconcentrator, gas chromatograph (GC), mass spectrometer (MS), and zero air/calibration system. All processes and data acquisition are computer controlled. The instrument is briefly described by Apel et al. (2010). Three traps are used: a water trap, an enrichment trap and a cryofocusing trap, with no adsorbents in any of the traps. The GC is a custom-designed unit that is lightweight and temperature programmable, fitted with a Restek MTX-624 column (I.D. = 0.18 µm, length = 8 m). Detection limits are compound dependent but range from sub-pptv (parts per trillion by volume) to 20 pptv. The system is calibrated with an in-house gravimetrically-prepared mixture containing 25 of the targeted 28 compounds. Post-mission calibrations were performed to obtain response factors for the three compounds not in the standard. The calibration mixture was dynamically diluted with scrubbed ambient (outside aircraft) air to mixing ratios near typically-observed levels.

The 28 VOCs observed by TOGA during ARCTAS include NMHC (C_4 and C_5 alkanes, isoprene, benzene, toluene, the C_8-aromatic VOCs), OVOCs (acetaldehyde (CH_3CHO), methanol (CH_3OH), ethanol (C_2H_5OH), acetone (CH_3COCH_3), propanal (C_3H_6O), methacrolein ($CH_2C(CH_3)CHO$), methyl vinyl ketone (MVK; $CH_2CHCOCH_3$), butanal (C_4H_8O), methyl ethyl ketone (MEK; $C_2H_5COCH_3$) methyl *tert*-butyl ether (MTBE; $C(CH_3)_3OCH_3$)), halogenated VOCs (chloromethane (CH_3Cl), bromomethane (CH_3Br), dichloromethane (CH_2Cl_2), chloroform ($CHCl_3$), tetrachloromethane (CCl_4)), acetonitrile (CH_3CN) and dimethylsulfide (DMS; CH_3SCH_3).

In addition to the TOGA, two other instruments on board the DC-8 measured some of the above VOCs as well as additional VOC mixing ratios: a proton-transfer-reaction

Title Page

Abstract | Introduction

Conclusions | References

Tables | Figures

◀ | ▶

◀ | ▶

Back | Close

Full Screen / Esc

Printer-friendly Version

Interactive Discussion

mass spectrometer (PTR-MS) and a whole air sampler (WAS). Recently, de Gouw and Warneke (2007) reviewed the use of PTR-MS for measurements of VOCs in the Earth's atmosphere. During ARCTAS, the University of Innsbruck PTR-MS routinely measured methanol (m/z 33; m/z being the mass-to-charge ratio of the detected protonated ion), acetonitrile (m/z 42), acetaldehyde (m/z 45), acetone (m/z 59), the sum of isoprene and furan (m/z 69), the sum of MVK and methacrolein (m/z 71), benzene (m/z 79) and toluene (m/z 93). 0.5-to-1 s average mixing ratios were reported approximately once each 5–10 s for most compounds. Due to a poorer signal-to-noise ratio, acetaldehyde mixing ratios were reported as 1-min averages. Periodic pre-flight and in-flight calibrations were performed using a VOC gas standard (prepared by AiR Environmental, Inc., Broomfield, CO) containing approximately 1 ppmv (parts per million by volume) of all target compounds (except furan and methacrolein) in compressed nitrogen (accuracy: ±5 %). The standard gas was dynamically diluted to ppbv (parts per billion by volume) levels. For zeroing, the PTR-MS inlet flow was periodically diverted through a heated Pt/Pd catalyst.

Whole air samples were collected during the flights through a forward facing non-heated SS inlet (1/4″) into electropolished SS flasks and pressurized to 40 psig with a metal bellows pump (Senior Flexonics, MB 602) analyzed afterwards in a laboratory by gas chromatography (GC). 168 canisters were available for each flight. The canister sampling frequency varied depending on location and altitude, and was typically a 1-min integrated sample every 3–5 min during horizontal flight legs, and every 1–2 min during vertical flight legs and plume encounters. Above 9 km above sea level (a.s.l.), the sample integration period increased with increasing altitude to >120 s above 11 km a.s.l. After collection, the canisters were transported back to the University of California, Irvine (UCI) laboratory and analyzed for 79 trace gases comprising NMHCs, halocarbons, DMS, alkyl nitrates, and OVOCs using five columns and three detection methods: mass spectrometry (MS), flame ionization detection (FID), and electron capture detection (ECD) as described by Simpson et al. (2010). The reported detection limits are 3 pptv for most NMHC, 5 pptv for methacrolein and MVK, and 20, 50,

and 100 pptv for ethanol, methanol, and acetone, respectively. All NMHCs were calibrated against whole air working standards, which had been calibrated against NIST and Scott Specialty Gases standards. The precision of the C_2–C_4 NMHC analysis was ±3 % when compared to NIST standards during the Non-Methane Hydrocarbon Intercomparison Experiment (NOMHICE) (Apel et al., 1994, 1999). Further details are given by Colman et al. (2001) and Simpson et al. (2010).

Other gas-phase species of interest to BB studies measured on board the DC-8 included hydrogen cyanide (HCN), carbon monoxide (CO) and carbon dioxide (CO_2). HCN was quantified in integrated 0.5-s sampling every 15 s by chemical ionization mass spectrometry (CIMS) via reaction with CF_3O^- directly in sampled ambient air and monitoring the product ion $m/z = 112$. Other corrections for the sensitivity are made by in-flight standard addition calibrations of H_2O_2 and HNO_3, also measured by the same CIMS system (Crounse et al., 2006) and proxied to laboratory calibrations of HCN. The detection limit ($S/N = 1$) is better than 15 pptv for moderate to low water vapor levels (H_2O mixing ratio ≤ 0.004) (Crounse et al., 2009). CO observations were made using a diode laser spectrometer and reported at 1 Hz using the method described by Sachse et al. (1988). CO_2 observations were made with a non-dispersive IR analyzer described previously (Vay et al., 2003) and were also reported at 1 Hz. All observed data from the ARCTAS study are publicly available at http://www-air.larc.nasa.gov.

2.2 Modeling

The NCAR Master Mechanism (MM) was used to simulate the chemical evolution of observed VOCs within BB plumes, and to contrast the chemistry between BB plumes originating from a region highly influenced by anthropogenic activities and one that is largely devoid of anthropogenic influence. The Master Mechanism is a 0-D model with detailed gas-phase chemistry consisting of $\approx$ 5000 reactions among $\approx$ 2000 chemical species combined with a box model solver (Madronich and Calvert, 1990; Madronich, 2006). Constrained inputs may include species of interest, emissions and temperature. The model computes the time-dependent chemical evolution of an air parcel initialized

with known composition. For these model runs, no additional emissions, dilution or heterogeneous processes were included. Photolysis rates are calculated using the Tropospheric Ultraviolet-Visible (TUV) model (Madronich and Flocke, 1999).

3 Results and discussion

3.1 Comparisons of VOC measurements

ARCTAS was the first study in which TOGA and PTR-MS measurements were made on board the DC-8, and there was significant overlap between the VOCs observed by TOGA and those measured by PTR-MS and/or WAS during the campaign. To accommodate the different sampling frequencies of the many instruments on the DC-8, several time-base merges of the reported data were generated in which reported observations were averaged over specific timescales, including a 1-min merge, a 1-s merge, and a TOGA merge. For the TOGA merge, observations with sampling times that overlapped the TOGA sampling period were averaged to the timescale of the reported TOGA observations. In this work, comparisons between reported TOGA observations and reported PTR-MS and WAS observations were made using the TOGA merge.

Comparison plots of the mixing ratios of compounds reported by both TOGA and PTR-MS are shown in Fig. 1. Likewise, similar plots for many of the VOCs measured by both TOGA and WAS are shown in Fig. 2. The solid lines in the plots in Figs. 1 and 2 are orthogonal distance regression (ODR) fits to the data, with slope and intercept shown on each plot. The dotted lines in each plot show $y = x$ for comparison. Most compounds reported by both TOGA and PTR-MS show good agreement, with all ODR slopes within ± 0.15 of unity. For isoprene, because the reported PTR-MS data includes furan, a compound with elevated mixing ratios in BB plumes, the ODR fit shown on the isoprene comparison plot excluded data points identified as BB (see Sect. 3.2). Isoprene data identified as BB are shown on the isoprene plot in Fig. 1 (black circles), and clearly indicate that in BB plumes, the majority of PTR-MS isoprene + furan data

are larger than the TOGA isoprene data. For some VOCs, the reported mixing ratios deviate at higher mixing ratios, with larger values reported from the PTR-MS measurement than by the TOGA measurement, in particular for acetonitrile and to a lesser extent methanol, acetone and the combined MVK + methacrolein. There are also deviations between the TOGA and PTR-MS at very low mixing ratios (<10 pptv) for toluene, benzene and acetaldehyde, with TOGA generally reporting slightly lower mixing ratios.

Good agreement is also observed between the results from TOGA and WAS for most VOCs (Fig. 2), with the majority of the ODR fits having slopes within ±0.20 of unity. Exceptions to this include acetone (slope 1.48 ± 0.03), MEK (slope 1.34 ± 0.02) and isopentane (slope 1.31 ± 0.09). For these three VOCs, the TOGA mixing ratios at higher concentrations are larger than those from the WAS system. This is in contrast to the benzene and toluene results, with the TOGA mixing ratios on average 21.5 % and 23.2 % lower, respectively, than those from WAS. However, overall the TOGA mixing ratios for benzene and toluene agreed well with the PTR-MS values, with slopes of 1.011 ± 0.007 and 0.979 ± 0.006, respectively. Although the OVOCs measured by TOGA and WAS compare reasonably well on average, the spread in some of the comparison plots is greater than most of the other plots in Figs. 1 and 2, including those for OVOCs observed by TOGA and PTR-MS.

The majority of the VOC observations from ARCTAS are at background or near-background mixing ratios, with many of the largest mixing ratios from encounters with fresh BB emissions. Because of the non-uniformity of gases in fresh fire plumes and the limited spatial extent of the plumes, the different integrated sampling times of the instruments contribute significantly to the differences in larger mixing ratios. An example of how sampling integration time impacts VOC measurements is shown in Fig. 3, a time-series plot of the benzene observations from a section of the 4 July 2008 flight in which the DC-8 sampled two narrow smoke plumes followed by a wider smoke plume. In Fig. 3, TOGA, PTR-MS and WAS benzene measurements are plotted according to their reported measurement timescales along with the 1-s [CO] observations and the 1-min merge GPS altitude. For the WAS and TOGA measurements, the bars indicate

ARCTAS VOCs: biomass burning enhancements

R. S. Hornbrook et al.

the start and stop times of the integrated sampling. For the WAS system, the sampling flow rate is variable, with higher flow rates into the evacuated canisters at the beginning of the sampling interval, and lower flow rates towards the end as the target fill pressure is reached. The flow rate for the TOGA sampling is controlled at a constant volumetric flow of 50 sccm (standard cubic centimeters per minute). Included on the plot are the TOGA-merge values for the PTR-MS and WAS measurements. In the first narrow plume at approximately 02:00:30 UTC, both the TOGA and WAS systems observed benzene mixing ratios well above the background concentrations. However, because the integrated sampling time for the WAS measurement was longer than that of the TOGA, it also included some of the background air (indicated by low [CO]) and the resulting WAS-reported benzene mixing ratio is lower than that reported by TOGA and PTR-MS. During the next narrow plume, the timing of WAS captured the plume, while TOGA sampled before and after, missing the narrow plume altogether. Here, the WAS measurement is not included in the TOGA merge because there was no overlap in the integrated sampling times. However in a very structured air mass, an overlap in the sampling periods of even a few seconds could result in very different concentrations being compared side-by-side in the TOGA merge. This is seen in the TOGA-merge data at 02:12:30 UTC in which the WAS benzene mixing ratio is more than double those of TOGA and PTR-MS. Here the WAS observation included a portion of a large plume and background air, and the TOGA measurement was primarily background air, hence the TOGA-merge WAS [benzene] is more than double that of TOGA and PTR-MS measurements. Because of these differences, where possible, many of the analyses in this work were performed on the observations from more than one VOC measurement technique to eliminate bias from individual techniques. With the exception of acetaldehyde, due to the longer PTR-MS averaging period, no sampling bias is expected for the comparison of TOGA and PTR-MS measurements using the TOGA-merge, as the PTR-MS observations are integrated within the TOGA sampling period.

◄◄ | ►►

◄ | ►

Back | Close

Full Screen / Esc

Printer-friendly Version

Interactive Discussion

3.2 Biomass burning plume identification

Maps of MODIS fire counts in Asia and North America in (a) April 2008 and (b) June and July 2008 are shown in Fig. 4. During both the spring and summer ARCTAS deployments, the DC-8 sampled air masses originating from the regions with strong BB emissions (Fuelberg et al., 2010). For this analysis, interceptions of fire emissions by the DC-8 were identified by elevated mixing ratios of CH_3CN, HCN and CO. HCN has been identified as a BB tracer (Lobert et al., 1990; Shim et al., 2007). CH_3CN has been also identified as an indicator of BB emissions that is not significantly enhanced in urban areas of the United States where other anthropogenic tracers are elevated (de Gouw et al., 2003, 2006). Because background mixing ratios of CH_3CN, HCN and CO are not constant throughout the regions covered during ARCTAS, plume identification was done using the 1-min merge and TOGA merge data files and hand-identifying time periods with elevated fire tracer mixing ratios ranging from one minute up to 2 h in duration. Generally, "elevated" refers to CH_3CN mixing ratios >200 pptv, HCN mixing ratios > 400 pptv, and CO mixing ratios >175 pptv, but in regions with lower background mixing ratios, long-range BB plumes with lower threshold mixing ratios were also sometimes identifiable above the background. Air masses sampled in urban regions with both elevated fire tracers and strongly-enhanced anthropogenic tracers (e.g., toluene, NO_x) were not included in this analysis to provide a more precise analysis of only biomass burning emissions and enhancements.

Figure 5 is a map of the DC-8 flights from ARCTAS-A, -B and -CARB over North America, with identified BB plume interceptions colored by the approximated age of each plume. Interceptions with individual BB plumes ranging from between one minute to two hours were attributed to source regions using back trajectories and plume ages were estimated based on back trajectories, aircraft altitude, and local fire information. Similar BB plume interceptions from individual flights were grouped according to source region and chemical composition, and the average plume group age was estimated. A total of 40 BB plume groups were identified from 15 flights. For each plume group,

the modified combustion efficiency (MCE), defined as $\Delta CO_2/(\Delta CO_2 + \Delta CO)$ (Ward and Radke, 1993), where Δ indicates an excess mixing ratio from the background, was determined from observations of CO and CO_2. The fire-average emission ratio $\Delta CO/\Delta CO_2$ was determined from a least-squares linear fit of the 1-s merge CO and

5   CO_2 data, and the rearranged relationship for MCE = $1/[(\Delta CO/\Delta CO_2) + 1]$ was used to calculate the MCE. The uncertainty of the MCE was determined using the standard error in the linear fit to the CO vs. CO_2 data. A summary of the BB plume groups with flight times of individual plume encounters, BB source region, estimated average plume age, and MCE for each group is listed in Table 1.

10 ## 3.3   VOC enhancements in biomass burning plumes

Commonly used to quantify the atmospheric impact of BB, emission ratios or enhancement ratios can be determined for trace gases emitted from BB or produced in a BB plume as it ages. An emission ratio (ER) is the molar ratio between two emitted compounds measured at a fire source, and is generally reported as $\Delta[X]/\Delta[Y]$ where $\Delta[X]$

15 and $\Delta[Y]$ refer to excess mixing ratios of the two species in the smoke minus the mixing ratio of those species in background air. Y can be any emitted compound, but is generally a useful smoke tracer such as CO or CO_2. By definition, ERs should only refer to fresh emissions, whereas an enhancement ratio, also referred to as a normalized excess mixing ratio (EMR), can refer to the enhancement of a compound X measured

20 downwind from a fire with respect to the enhancement of a smoke tracer Y, also reported as $\Delta[X]/\Delta[Y]$. For shorter-lived VOCs such as ethene and toluene, EMRs observed downwind of a fire may be significantly lower than the ERs at the source. VOCs that are oxidation products of compounds emitted during BB may exhibit higher EMRs downwind of the fire, due to oxidative processing within the plume. Compar-

25 isons of EMRs of these compounds to those of longer-lived primary emissions such as benzene have been used to approximate plume age, based on relative reaction rates (de Gouw et al., 2006). In this work, we use the term excess mixing ratio (EMR) as

many of our observations occur far from the fire sources, but for many VOC EMRs in BB plumes < 0.2 days old, these may also be considered to be molar emission ratios or ERs.

Individual EMRs with respect to CO were determined for each plume group in Table 1 for a number of VOCs measured on board the DC-8 during ARCTAS. For each VOC X measured during the time period(s) for each plume group, $\Delta[X]/\Delta[CO]$ was determined from the linear least-squares fit to a plot of $[X]$ (pptv) against $[CO]$ in ppbv. CO mixing ratios corresponding to each reported measurement in the TOGA merge were used to determine EMRs from the TOGA observations. Likewise, the CO mixing ratios in the 1-min merge corresponding to each 1-min average PTR-MS, WAS and HCN measurement were used to determine EMRs for species of interest from those observations. EMRs are not reported for correlation plots of $[X]$ to $[CO]$ with $R^2 < 0.5$ or where VOC measurements were not available during the time period(s) specified for a particular plume group. For correlations of VOCs to CO with $R^2 > 0.5$, EMRs are listed in Table 2 with 1σ standard errors from the uncertainties in the slopes. The measured EMRs from the 40 plume groups were also plotted against estimated average plume age for each VOC, shown in Fig. 6. In these plots, each data point is colored by the primary BB source region: Alaska, Asia (Spring), Asia (Summer), California or Canada.

The mean EMRs to CO for HCN, CH_3CN and several OVOCs from each of the three major BB source regions measured during ARCTAS (i.e.: Asia, California and Canada) are summarized in Table 3, along with literature EMRs from several previous field studies. Likewise, a summary of the mean EMRs to CO for several NMHC is presented in Table 4 with literature values for comparison.

3.3.1 HCN

The mean HCN to CO EMR observed during ARCTAS is 7.0 ± 3.8 pptv ppbv^{-1} (1σ standard deviation), with an order of magnitude of variability, ranging from 1.56 ± 0.09 to 15.1 ± 1.0 pptv ppbv^{-1}. CO and HCN have tropospheric lifetimes of approximately

two months (Fisher et al., 2010) and a few months, respectively, with BB as the primary source and ocean uptake as the primary sink of HCN (Li et al., 2000). In contrast, the primary sink for CO is reaction with the OH radical. The ratio of HCN to CO in a BB plume would therefore be relatively unchanged over the first 10 days after emissions, provided there is little dilution with air masses having different HCN to CO ratios yet significant amounts of one or the other (e.g.: a concentrated urban plume). As shown in Fig. 6, with the exception of the Californian BB, the range of HCN EMRs observed during ARCTAS is not dependent on the average age of the BB plume. Nevertheless, the scatter in the measurements indicates that there is significant variability in HCN to CO molar emission ratios. Although Δ[HCN]/Δ[CO] EMRs from the Californian BB appear to increase with plume age, the single data point greater than 3 days old was observed over the Saskatchewan/Alberta region. Given the impact of local Canadian BB emissions convected into the mid-troposphere (Alvarado et al., 2010), it is possible that the HCN and CO observed were from a mixture of Californian and Canadian BB emissions.

Observed HCN EMRs from California fires during ARCTAS-CARB were significantly lower than those from Canadian or Asian fires during spring and summer 2008. The mean HCN to CO EMRs from the Asian BB, Californian BB and Canadian BB are 8.8 ± 3.8, 3.1 ± 1.9 and 7.6 ± 3.2 pptv ppbv^{-1}, respectively. From Table 3, previous measurements of HCN EMRs to CO also vary widely. Andreae and Merlet (2001) reported literature averages for three primary BB source regions: African Savanna, tropical forest and extratropical forests: 0.43, 1.5 and 1.4 pptv ppbv^{-1}, respectively. EMRs measured by Sinha et al. (2003, 2004) in African savannas were much higher, with average values between 6 and 9 pptv ppbv^{-1}. Similarly, Yokelson et al. (2007a, 2009) reported HCN to CO EMRs from two tropical forest regions in the Yucatan and Brazil averaging between 6.6 and 7.0, but with high variability. As well, Yokelson et al. (2007b) reported HCN EMRs in the Mexico City region of 12 ± 7 pptv ppbv^{-1}. This high average HCN EMR was attributed to high NO$_x$ deposition in the mountains surrounding Mexico City and the authors suggested that there may be similarly high ratios near the LA Basin.

However, the HCN EMRs measured in California were on average the smallest values observed during the ARCTAS study, and are much lower than the average EMR from the Mexico City region. It should be noted that most of the wildfires in California during June 2008 were north of the Los Angeles region, primarily in the northern region of California's Central Valley (Fig. 5b), which is likely less impacted by LA NO_x pollution than the mountains immediately surrounding the LA Basin.

The Asian and Canadian fires were primarily in boreal forests, whereas the majority of the Californian BB was in regions with sage brush vegetation. The differences in the measured HCN EMRs could be indicative of the different fuels and fire conditions in Siberia and Canada compared to those in California.

3.3.2 Acetonitrile

As shown in Table 3, reported EMRs for $\Delta[CH_3CN]/\Delta[CO]$ typically range between 1.2 and 4.3 pptv ppbv^{-1}. The mean CH_3CN to CO EMR observed during ARTCAS is 1.5 ± 0.6 pptv ppbv^{-1} using the TOGA CH_3CN data, and 1.7 ± 0.6 pptv ppbv^{-1} using the PTR-MS CH_3CN, both within the range of previously reported values but certainly on the low end. Separating the data by source region, the mean observed EMRs from the Asian, Californian and Canadian BB are 1.4 ± 0.4, 1.4 ± 0.7 and 1.7 ± 0.4 (all pptv ppbv^{-1}), respectively, using the TOGA CH_3CN measurements, and 1.4 ± 0.5, 1.7 ± 0.6, and 1.8 ± 0.3 (pptv ppbv^{-1}) using the PTR-MS CH_3CN data. Unlike HCN, the observations from ARCTAS suggest that CH_3CN to CO emission ratios do not vary significantly between the BB source regions sampled. Additionally, both the overall mean EMR and the regional mean EMRs are statistically equivalent using CH_3CN data from either the TOGA or PTR-MS. For the remainder of the VOC EMRs discussed in Sect. 3.3, unless noted due to significant differences between the measurements, we refer to EMRs determined using the TOGA data for compounds in which TOGA measurements exist.

From previous field studies, CH_3CN EMRs to HCN have been fairly consistent: 0.39 in the Mexico City region (Crounse et al., 2009), 0.41 from Brazil deforestation (Yokelson et al., 2008) and 0.43 in the Yucatan region (Yokelson et al., 2009). From this work, the CH_3CN to HCN EMRs from individual plume groups range from 0.10 to 0.66, with a mean of 0.22 ± 0.10. Separated by source region, the mean CH_3CN to HCN EMRs are 0.15 ± 0.04, 0.32 ± 0.13 and 0.24 ± 0.07 for Asian, Californian and Canadian source regions. The lifetime of CH_3CN in the troposphere is on the order of months, with the primary loss via reaction with OH and ocean uptake (de Gouw et al., 2003). Although the lower mean from the Asian fires could point to ocean uptake of CH_3CN, the difference between the regional mean CH_3CN to HCN EMRs are more likely due to variability in HCN emissions, based on the relative emission ratios to CO. Even accounting for loss to the ocean, most of the long-range Asian BB plumes sampled during ARCTAS were lofted into the mid- to upper-troposphere, and thus significant changes are not expected in the EMRs within 10 days of emissions. Overall, there is less variability in CH_3CN EMRs to CO than to HCN due to the variability in the HCN emissions.

3.3.3 Oxygenated VOCs

The EMRs of acetone to CO observed during ACTAS are highly variable, ranging between 1.7 ± 0.7 and 16 ± 1 pptv ppbv^{-1}, with a mean EMR of 7.4 ± 4.0 pptv ppbv^{-1}. Separated by source region, the mean EMRs are 9.0 ± 3.6, 6.0 ± 3.8, and 5.9 ± 4.0, all pptv ppbv^{-1}, from Asian, Californian and Canadian BB, respectively. Jost et al. (2003) reported an increase in acetone EMRs to CO in an aging fire plume over a much shorter timescale, ranging from 4.8 pptv ppbv^{-1} in a fire plume estimated to be 17 min old to 11.3 pptv ppbv^{-1} downwind in the same fire plume estimated to be 125 min old. Other literature values for Δ[acetone]/Δ[CO] EMRs range between 1.5 pptv ppbv^{-1} (Holzinger et al., 2005) and 1.7–2.1 pptv ppbv^{-1} (Friedli et al., 2001) in very young fire plumes to 19.5 pptv ppbv^{-1} (Andreae and Merlet, 2001) and 20–30 pptv ppbv^{-1} (Singh et al., 1994) in aged biomass burning plumes. From Fig. 6, there is no appreciable

increase or decrease in the acetone EMRs with plume age from the ARCTAS results, although is certainly significant variability in the observations.

The acetaldehyde to CO EMRs observed during ARCTAS range from as high as 22 pptv ppbv^{-1}, measured by both TOGA and PTR-MS in a fresh California BB plume, to less than 2 pptv ppbv^{-1} in several long-range Asian BB plumes measured by the PTR-MS during the spring campaign. For shorter-lived VOCs, observed EMRs decrease as plume age increases. In the acetaldehyde plot in Fig. 6 there is a decrease in the observed EMRs as BB plume age increases. Although a number of Asian BB plumes were sampled during both the spring and summer campaigns, of those estimated to be more than four days old only a few of the spring BB plumes contained sufficient acetaldehyde to determine the EMR, averaging 1.2 ± 0.3 pptv ppbv^{-1}. Mean acetaldehyde to CO EMRs from younger Californian and Canadian BB were 6.0 ± 3.8 and 5.9 ± 4.0 pptv ppbv^{-1}, respectively. Acetaldehyde has a tropospheric lifetime of approximately 1 day with the primary loss due to reaction with OH. Thus, the increased average [OH] in summer months at mid- to high-latitudes is the most likely reason long-range acetaldehyde EMRs were not observed in the summer, rather than a difference in emission ratios between the spring and summer fires. Observable differences between the spring and summer EMRs in Asian BB were seen for a number of other VOCs, including MEK, benzene, toluene, and the C_2–C_5 alkanes, and are likely also due to increased OH loss rates of these VOCs during the summer months.

Literature observations of acetaldehyde EMRs and emission ratios also vary widely. Yokelson et al. (2007a) reported acetaldehyde EMRs to CO of 8.7 ± 5.1 pptv ppbv^{-1} from deforestation fires in Brazil and 18.7 pptv ppbv^{-1} from fresh fire emissions in the Yucatan (Yokelson et al., 2009), while de Gouw et al. (2006) reported acetaldehyde EMRs well below 2 pptv ppbv^{-1} in aged Alaskan and western Canada BB plumes sampled over the Northeastern United States. In the latter, the relative ratios of acetaldehyde and benzene EMRs to CO indicated secondary production of acetaldehyde within the BB plumes.

ARCTAS VOCs: biomass burning enhancements

R. S. Hornbrook et al.

Title Page

Abstract	Introduction
Conclusions	References
Tables	Figures

|◄ | ►|

◄ | ►

Back | Close

Full Screen / Esc

Printer-friendly Version

Interactive Discussion

The methanol EMRs to CO observed during ARCTAS range between 5 and 54 pptv ppbv^{-1}, with a mean of 19 ± 12 pptv ppbv^{-1}. By source region, the mean methanol EMRs of 21 ± 10, 21 ± 15 and 18 ± 14, all pptv ppbv^{-1}, in Asian, Californian and Canadian BB plumes, respectively, indicate very little difference between source region and plume age. Unlike acetone, little photochemical production of methanol is expected. Published EMRs of methanol to CO vary widely, ranging between 1.8 (Friedli et al., 2001) and 27 pptv ppbv^{-1} (Yokelson et al., 2009), while the majority lie between 10 and 25 pptv ppbv^{-1}.

Using the TOGA ethanol observations, EMRs to CO ranging from 0.25 ± 0.04 to 4.5 ± 0.5 pptv ppbv^{-1} were observed during ARCTAS, primarily from fresh Canadian and Californian BB. Fewer ethanol EMRs could be determined using the WAS measurements (Table 2), ranging from 0.38 ± 0.08 to 2.6 ± 0.2 pptv ppbv^{-1}. To the authors' knowledge, the only published ethanol BB data are four emission factors ranging between 0.002 ± 0.002 and 0.051 ± 0.139 g kg^{-1} (grams of ethanol per kilogram of dry matter burned) (Ciccioli et al., 2001), and 0.018 g kg^{-1} (Andreae and Merlet, 2001), corresponding to a molar emission ratio to CO of 0.10 pptv ppbv^{-1}. The values reported by Ciccioli and coauthors were obtained in laboratory experiments with two different fuels in both flaming and smoldering stages. The value reported by Andreae and Merlet was determined from canister samples in which wall losses may have been a factor. The smallest EMR observed during ARCTAS is in agreement with the published values, but the mean of 1.5 ± 1.4 pptv ppbv^{-1} (using both TOGA and WAS data) indicates that BB emission ratios of ethanol to CO are highly variable, and range up to an order of magnitude larger than previous measurements. Thus, emission inventories based on previously-published measurements may significantly underestimate the magnitude of fire-emitted ethanol.

The MEK EMRs observed during ARCTAS range between 0.21 and 2.2 pptv ppbv^{-1} with a mean EMR of 0.65 ± 0.41 pptv ppbv^{-1}, similar to published MEK EMRs to CO which range between 0.7 and 3.0 pptv ppbv^{-1} (Table 3). Separated by source region, the respective mean MEK EMRs from Asian, Californian and Canadian BB of

ARCTAS VOCs: biomass burning enhancements

R. S. Hornbrook et al.

Title Page

Abstract	Introduction
Conclusions	References
Tables	Figures

⏮   ⏭

◀   ▶

Back   Close

Full Screen / Esc

Printer-friendly Version

Interactive Discussion

0.56 ± 0.11, 0.82 ± 0.54 and 0.66 ± 0.58 pptv ppbv^{-1}, are statistically equivalent, with no clear dependence on BB plume age or source region. There is, however, a statistical difference between the spring and summer Asian BB EMRs: 0.9 ± 0.2 and 0.29 ± 0.07 pptv ppbv^{-1}, respectively. The MEK OH rate coefficient is approximately 1.22 × 10^{-12} cm^3 molecule^{-1} s^{-1} (Atkinson and Arey, 2003) and the photolytic lifetime is estimated to be on the same order of magnitude as OH-removal (Raber and Moortgat, 1995; Atkinson, 2000). Thus, the difference in the MEK tropospheric lifetime between the spring and summer months is the likely reason for the difference in the observed EMRs.

The MVK to CO EMRs observed during ARCTAS range between 0.2 and 6 pptv ppbv^{-1}, with mean EMRs of 0.70 ± 0.34 and 1.6 ± 2.1 pptv ppbv^{-1} from Californian and Canadian BB, respectively. The observed methacrolein EMRs to CO range between 0.10 and 3.1 pptv ppbv^{-1}, with respective mean EMRs to CO of 0.5 ± 0.2 and 1.0 ± 1.1 pptv ppbv^{-1} from Californian and Canadian BB. Few EMRs for these isoprene oxidation products have been published. Yokelson et al. (2007a) reported an EMR to CO for the sum of MVK + methacrolein of 1.9 ± 0.7 pptv ppbv^{-1} from Brazilian deforestation fires. Recently, Yuan et al. (2010) reported an EMR for the sum of MVK + methacrolein to CH$_3$CN of 2.3 ± 0.8 (pptv pptv^{-1}) in the Pearl River Delta (PRD) region of China. Applying our mean EMR for CH$_3$CN to CO of 1.5 ± 0.6 pptv ppbv^{-1}, we estimate the PRD EMR to CO at 3.5 ± 1.8 pptv ppbv^{-1}. Combined, the MVK + methacrolein EMRs from fresh Californian and Canadian BB range between 0.31 ± 0.05 and 10 ± 2 pptv ppbv^{-1}, with a mean value of 2.1 ± 2.7 pptv ppbv^{-1}, in agreement with the few published values.

In addition to MVK and methacrolein, isoprene was observed in several BB plumes, with EMRs to CO ranging from 0.14 ± 0.07 to 9 ± 2 pptv ppbv^{-1}. Isoprene enhancement ratios have been previously reported, but because the tropospheric lifetime of isoprene is so short (i.e., a few hours or less) it is difficult to extract meaning from enhancement ratio observations. It is unclear from the observations during ARCTAS whether the isoprene enhancements in identified BB plumes are due to natural emissions or

biomass burning. Regardless of the origin of the emissions, because of the very short atmospheric lifetime of isoprene, it is rare to see significant concentrations of isoprene in the upper troposphere. During ARCTAS, there were several occasions during which significant isoprene mixing ratios were observed above 8 km, most likely as a result of strong BB-influenced convection over Central Canada. These convective events and the impact of reactive isoprene on the HO_x budget of the upper troposphere are explored in another paper from our group (Apel et al., 2011).

3.3.4 Alkanes

The ethane to CO EMRs observed during ARCTAS range between 2.7 ± 0.7 and 19 ± 3 pptv ppbv^{-1}, with a mean value of 6.1 ± 3.2 pptv ppbv^{-1}, similar to published values (Table 4), which range between 1.7 ± 0.1 pptv ppbv^{-1} (Sinha et al., 2004) and 10.8 ± 6.6 pptv ppbv^{-1} (Andreae and Merlet, 2001). As with MEK, there is a clear difference between the mean ethane EMRs observed in Asian BB plumes during the spring and summer campaigns, 7.8 ± 2.4 and 4.3 ± 1.4 pptv ppbv^{-1}, respectively.

The observed EMR for ethane to CO of 19 ± 3 pptv ppbv^{-1} is from plume group 28, a fresh Canadian BB plume sampled during the 4 July 2008 flight. Relative to the other groups, plume group 28 contained significantly higher alkane to CO enhancement ratios, as well as above-average EMRs for MVK, methacrolein, acetone, methanol and ethanol. Although the air mass sampled during this time had elevated BB tracers (i.e., CO, HCN and CH_3CN), the magnitude of each fire tracer was small in comparison to other fresh plumes sampled during ARCTAS. The MCE of plume group 28, 1.01 ± 0.01, is higher than the majority of the fresh (< 0.5 days old) Canadian BB plumes sampled, which had a mean MCE of 0.91 ± 0.03. An MCE of approximately 1.0 suggests that this is a BB plume from a fire in a pure flaming stage in which emission ratios to CO are high due to overall low CO emissions. However, it is conceivable that emissions from non-BB sources were impacting the air mass. This region of Central Canada is well known for oil and natural gas extraction (Simpson et al., 2010), and a high proportion of C_2–C_4 alkanes in comparison to unsaturated C_2–C_4 NMHC is indicative of natural gas

extraction (Katzenstein et al., 2003). Figure 7 is a plot of the average mixing ratios of selected C_2–C_6 NMHC (using only WAS observations, for internal consistency) in four different fresh Canadian BB plume groups including plume group 28. The plot clearly shows that plume group 28 has a very different proportion of saturated and unsaturated

5 NMHC.

Published propane to CO EMRs range from 0.25 ± 0.10 (Sinha et al., 2004) to 3.0 ± 4.0 pptv ppbv^{-1} (Yokelson et al., 2007b). The propane EMRs observed during ARCTAS vary between 0.7 ± 0.2 and 17 ± 3 pptv ppbv^{-1}, with a mean of 2.6 ± 3.5 pptv ppbv^{-1}. Again, the largest observed propane EMR was from plume group 28. The next highest

10 value was significantly lower (3.8 ± 0.7 pptv ppbv^{-1}), so excluding the point from plume group 28 results in an overall mean propane EMR of 1.8 ± 0.8 pptv ppbv^{-1}, with statistically no difference between the mean EMRs for Asian, Californian and Canadian BB sources, as shown in Table 4 and is in agreement with published values for extratropical forests. Separating the Asian EMRs into spring and summer observations,

15 the mean EMRs are 2.8 ± 1.1 and 1.5 ± 0.3 pptv ppbv^{-1}, respectively, most likely due to differences in OH-removal rates.

Published isobutane to CO EMRs range between 0.01 (Sinha et al., 2004) and 0.39 ± 0.46 pptv ppbv^{-1} (Yokelson et al., 2007b). With the exception of the isobutane EMR from plume group 28 (2.4 ± 0.2 pptv ppbv^{-1}), the relative enhancements observed

20 during ARCTAS are all within the range of previously reported values, with a mean of 0.33 ± 0.53 pptv ppbv^{-1} including the high value, and 0.22 ± 0.20 pptv ppbv^{-1} excluding the data point. Likewise, published *n*-butane to CO EMRs range between 0.06 ± 0.01 (Sinha et al., 2004) and 1.1 ± 1.2 (Yokelson et al., 2007b), both pptv ppbv^{-1}, and the EMRs observed during ARCTAS fall within this range with the exception of the EMR

25 from plume group 28 (5.1 ± 0.7 pptv ppbv^{-1}), with overall mean EMRs of 0.65 ± 0.97 and 0.46 ± 0.29 pptv ppbv^{-1}, including and excluding the high value, respectively. As shown in Table 4, the EMRs for isopentane and *n*-pentane also fall within the range of previously published values.

3.3.5 Aromatic hydrocarbons

The observed benzene to CO EMRs during ARCTAS are quite consistent, regardless of source, and although they range between 0.63 ± 0.05 and 2.2 ± 0.2 pptv ppbv^{-1}, the overall mean is 1.2 ± 0.3 pptv ppbv^{-1}. By source region, the mean benzene to CO EMRs are 0.96 ± 0.21, 1.2 ± 0.3 and 1.4 ± 0.4 pptv ppbv^{-1} for Asian, Californian and Canadian BB, respectively. Although the means are not statistically different, there is a slight separation between the Asian BB EMRs observed during the spring and summer: 1.1 ± 0.2 and 0.8 ± 0.2 pptv ppbv^{-1}, respectively. From the literature EMRs in Table 3, with the exception of the reported average benzene EMR from observations in smoke plumes in the Yucatan (Yokelson et al., 2009) (3.4 ± 0.8 pptv ppbv^{-1}), the published benzene EMRs in Table 4 are all between 0.65 ± 0.01 and 1.6 ± 0.6 pptv ppbv^{-1}.

The literature values for toluene EMRs to CO shown in Table 4 range between 0.18 and 1.3 pptv ppbv^{-1}. During ARCTAS, the observed toluene EMRs ranged between 0.12 ± 0.03 and 0.85 ± 0.02 pptv ppbv^{-1}, with an overall mean of 0.51 ± 0.18 pptv ppbv^{-1}. As a relatively short-lived species with respect to CO, Δ[toluene]/Δ[CO] EMRs decrease with increasing plume age, as shown in Fig. 6, although there is also a significant spread in the observed values in young BB plumes. The mean regional EMRs for Asian, Californian and Canadian BB, 0.12 ± 0.03, 0.51 ± 0.19 and 0.57 ± 0.09 pptv ppbv^{-1}, respectively, indicate a significant decrease in the Asian BB toluene EMRs between emission and sampling, and no statistical difference between Canada and Californian toluene BB.

Published values for C_8-aromatics EMRs with respect to CO range between 0.15 ± 0.07 pptv ppbv^{-1} (Andreae and Merlet, 2001) and 0.55 ± 0.27 pptv ppbv^{-1} for the combined ethylbenzene + p-, + m- + o-xylene (Yokelson et al., 2007a). The observed EMRs (from Californian and Canadian BB only) are on the lower end of the published values, ranging from 0.012 ± 0.002 (o-xylene) to 0.20 ± 0.04 (ethylbenzene + p- and m-xylene) pptv ppbv^{-1}, and having a mean of 0.08 ± 0.05 pptv ppbv^{-1} for ethylbenzene, p- + m-xylene, and 0.06 ± 0.05 pptv ppbv^{-1} for o-xylene, and no statistical difference between Californian and Canadian BB EMRs.

3.4 Evolution of VOCs in biomass burning plumes

Gas-phase VOCs are often loosely classified as primary VOCs and secondary VOCs. Primary VOCs consist of NMHC and OVOCs emitted directly into the atmosphere, while secondary VOCs include OVOCs, organic nitrates and particulate organic matter, and are formed in the troposphere from the photo-oxidization of primary VOCs. Many species of OVOCs are believed to exist as both primary and secondary VOC, but uncertainties remain regarding the relative contribution to the total OVOC for a given species based on source type and photochemical age. The evolution of OVOCs in some anthropogenic air masses has been investigated, for example, secondary production of acetaldehyde has been shown to be important in urban outflow (de Gouw et al., 2005; Apel et al., 2010). There have also been indications that OVOC production may be significant in BB plumes, as noted by de Gouw et al. (2006) based on comparisons of observed acetaldehyde to benzene EMRs in aged boreal forest fire plumes. As discussed in Sect. 3.3.3, acetone EMRs to CO have been reported to increase in aging fire plumes over short timescales (i.e. hours) (Jost et al., 2003), and literature EMRs from aged BB plumes seem to indicate that over longer timescales, acetone EMRs to CO continue to increase.

The evolution of VOCs within BB plumes observed during ARCTAS was investigated using the NCAR Master Mechanism. Two sets of initial conditions were used to model the chemical evolution of trace gas-phase chemical species over 2.5 days within a BB plume. The initial conditions were based on observations from ARCTAS-CARB and ARCTAS-B of a fresh BB plume in California (CAL BB) and a fresh BB plume in Central Canada (CAN BB), and initialized at noon on day 1. The conditions for the CAL BB model run were more "polluted" than the CAN BB model run, with 4× larger CO and VOCs, an order of magnitude larger NO_x, twice the O_3, and 1.4× the OH. Although VOC mixing ratios were 4× larger in the CAL BB run, the relative mixing ratios of different classes of VOCs in these starting conditions are similar, as shown in Fig. 8a, b.

Title Page

Abstract | Introduction

Conclusions | References

Tables | Figures

◄ | ►

◄ | ►

Back | Close

Full Screen / Esc

Printer-friendly Version

Interactive Discussion

In both the Canadian BB and Californian BB initial conditions, OVOCs comprise approximately 65 % of the VOCs in the plume. In contrast, Fig. 8c, the distribution of the same classes of VOCs observed in an urban region during ARCTAS, shows that OVOCs comprise less than 50 % of observed VOCs. Ratios of OVOC/VOC ranging from 60–80 % have been observed in BB emissions (Yokelson et al., 2008, 2009; Burling et al., 2010), and are higher than OVOC/VOC ratios observed in air masses primarily influenced by fossil fuel burning emissions, typically less than 50 % (de Gouw et al., 2009; Apel et al., 2010). It should be noted that these percentages rely heavily on the compounds included. Compound classes in Fig. 8 are comprised of C_2–C_6 alkanes (alkanes); C_2–C_4 alkenes, isoprene, α- and β-pinene (alkenes); ethyne and propyne (alkynes) C_6–C_8 aromatics (aromatics); C_1–C_4 aldehydes (aldehydes); acetone, MEK, MVK (ketones); and C_1–C_2 alcohols (alcohols). Inclusion of other compounds (e.g., alkyl nitrates and halogenated VOCs) would change the absolute ratio, but the relative difference between the OVOC/VOC ratios in the two BB plumes and the anthropogenically-influenced air masses would still exist. With smaller relative concentrations of NMHC precursors and a higher proportion of OVOCs, the chemistry within BB plumes is likely to differ from that of anthropogenic plumes.

From the CAN BB and CAL BB model results, most OVOC mixing ratios decrease with age within the BB plumes, indicating OVOC loss reactions within the BB plumes are greater than any production terms. The only exceptions to this are the isoprene oxidation products MVK and methacrolein during the CAN BB model run, which increase for approximately 3–4 h while isoprene is still present in significant amounts (i.e., >300 pptv), and then decrease for the remainder of the run. Figure 9 shows plots of the changes of nine VOCs EMRs to CO over 2.5 days for both model runs. For comparison, observed EMRs from the TOGA observations in BB plumes estimated to be three days in age or less are also plotted in Fig. 9 according to the estimated BB plume age. In both model runs, all VOC ratios to CO are predicted to decrease over a period of 2.5 days, with the exception of the MVK EMR (and the methacrolein EMR, which is not plotted but has similar behavior to MVK) during the first few hours of the CAN BB

model run. As expected, for isoprene, toluene, and acetaldehyde (tropospheric lifetimes approximately 1 day or less), there is a fairly rapid daylight-dependent decrease in the modeled EMRs, while for some of the OVOCs with tropospheric lifetimes approximately 1 week or greater (i.e., methanol, acetone, MEK) the modeled EMRs remain fairly constant with time, decreasing only slightly over 2.5 days.

For most VOCs in Fig. 9, the observed EMRs in fresh BB (< 1 day) are highly variable, with some observed EMRs significantly larger than the conditions chosen for the model runs. By the time the plumes are estimated to be 1.5 to 2 days in age, the majority of the observed EMRs are in relatively good agreement with the modeled EMRs. However, for acetone, methanol, MEK, and to a lesser extent, benzene and ethanol, the EMRs to CO are not predicted to change significantly over 2.5 days, suggesting that any variability in fresh BB emissions is likely to be maintained in an aging plume.

Overall there are few differences evident between the chemical evolution of VOCs in BB plumes in the "more-polluted" CAL BB (with disproportionately higher VOC, NO_x and O_3 concentrations) and the "less-polluted" CAN BB based on the two model runs. There are generally higher toluene EMRs evident in both the observations and model run for Californian BB plumes and, similarly, there are higher isoprene and MVK EMRs in the observations and the model run for Canadian BB plumes. Although the EMRs for acetone and ethanol in the two box model runs are initialized at different values, the relative evolutions of these EMRs in the two types of aging BB plumes are similar.

3.5 Ratios of light alkane enhancements

Comparison plots of the observed EMRs to CO for several light alkanes versus the co-observed propane to CO EMR are shown in Fig. 10. For the plots comparing ethane, *n*-butane, isobutane and *n*-pentane to propane, the data from plume group 28 is shown (Fig. 10a, c, e, g), and a second, detailed plot of the remaining data for each of these NMHCs is also included (Fig. 10b, d, f, h). Because the data from plume group 28 would skew the results significantly, these data are not included in the fits discussed below. In general, the ratios to CO of these light alkanes are not strongly correlated

with the estimated photochemical age of the BB plume, though a range of EMRs were observed for each VOC during ARCTAS. Included on each comparison plot in Fig. 10 is a linear fit to the observed ARCTAS data, excluding the high EMR values from plume group 28. Also included on each plot are the equivalent literature ratios from Table 4.

Figure 10a and b are comparison plots of ethane and propane EMRs to CO. The fit to the observed ARCTAS data has a slope of 2.6 ± 0.3 and an R^2 value of 0.81, with only a few of the literature ratios deviating significantly from the fit, shown clearly in Fig. 10b. The well-correlated linear fit to the EMR data suggest that ethane and propane emissions from fires are strongly correlated. Figure 10c and d are comparison plots of n-butane and propane EMRs to CO. Similar to the ethane versus propane plot, the linear fit to the observed n-butane vs. propane EMRs indicates fairly good correlation with a slope of 0.23 ± 0.05, and an R^2 value of 0.66. As well, the majority of the literature values on the plots are well described by the linear fit, the exception being the ratio of the EMRs observed by Yokelson et al. (2007b) from fires in the Mexico City (MC) region. The next two plots, Fig. 10e, f, show the EMR comparison for isobutane and propane. The linear fit to the data indicates good correlation between isobutane and propane emissions, with a slope 0.19 ± 0.03 and an R^2 value of 0.82. The last three plots in Fig. 10 are comparison plots of n-pentane (g and h) and isopentane (i) EMRs to the observed propane EMRs. For the n-pentane EMRs, the linear fit to the ARCTAS data has an R^2 value of 0.23, indicating no clear correlation. In Fig. 10i, however, the linear fit to the isopentane and propane data has a slope of 0.12 ± 0.02 and R^2 value 0.79. Overall, with the exception of the n-pentane data, with lower observed mixing ratios resulting in higher uncertainties in the correlation plots, our observations suggest strong correlations between the emissions of light C_2–C_5 alkanes from fires.

4   Conclusions

During the ARCTAS campaign, instruments on board the NASA DC-8 measured the mixing ratios of a large number of VOCs in BB plumes originating from several fires burning in Asia and North America ranging from fresh emissions to plumes over a week in age. Of the VOCs measured by TOGA, several were co-observed by other measurement techniques. There was very good agreement between the instruments for the majority of the flights and, in general, quantitative differences between the systems can be explained by the different sampling integration times of the instruments, particularly in highly variable air masses such as those encountered in fresh BB emissions.

For our analysis, BB plume encounters by the DC-8 were grouped by flight, plume age and source region into 40 individual plume groups for analysis. EMRs to CO were determined for HCN, acetonitrile, several NMHC and OVOCs for each of the plume groups, and compared to literature values. Overall, the EMRs observed during ARCTAS showed good agreement with literature values for most VOCs. For some compounds, however, such as ethanol, MVK and methacrolein, very few literature values have been published. For example, the ethanol to CO EMRs observed during ARCTAS range from values similar to the three previously-reported EMRs ($0.1 \, \mathrm{pptv \, ppbv^{-1}}$) to well over an order of magnitude larger ($4.5 \pm 0.5 \, \mathrm{ppt \, ppbv^{-1}}$). Such a wide range in observed EMRs is common for most VOCs discussed here, with literature EMRs varying up to an order of magnitude, depending on the BB source region, fuel type, and plume age. Although observed in other studies, this variability is often diluted in the literature when observations from several plumes are averaged together to generate an overall regional EMR from a particular study. The result of this is a perception that EMRs are reliably consistent from a particular region or fuel type, and this is not necessarily the case, as our results have shown. For some compounds, this may lead to significant under- or over-prediction of emissions in fire emissions inventories.

Using two sets of initial BB plume conditions based on observations made on board the DC-8 in both fresh Californian and fresh Canadian BB emissions, the NCAR Master

Mechanism was used to model the chemical evolution of VOCs and VOC to CO in a BB plume over 2.5 days. The results from these box model simulations were compared to ARCTAS-observed EMRs. The Californian BB plume was significantly more polluted than the Canadian BB plume, with 10× greater NO_x, twice the O_3 concentrations, and 4× greater VOC and CO concentrations. However, apart from higher toluene EMRs in the Californian BB plume, and higher isoprene and isoprene reaction product EMRs in the Canadian BB plume, there were few differences between the plumes in terms of relative ratios of VOCs to CO with time. Although the concentrations of MVK and methacrolein are predicted to increase slightly while isoprene is still present in significant amounts (>300 pptv), all OVOCs observed by TOGA are predicted to decrease over a period of 2.5 days within the plumes. As well, all EMRs to CO for OVOCs observed by TOGA are predicted to decrease over the 2.5 days. Although they generally decrease with time, the time-dependences of the modeled EMRs of acetone, methanol and MEK, and to a smaller extent, ethanol, are relatively flat, indicating that much of the variability in observed EMRs to CO in BB plumes are due to variability in the emissions.

Although significant variability exists in observed EMRs from both ARCTAS and previous field studies, some VOCs have EMRs to CO that are highly correlated. This was clearly shown for the light C_2–C_5 alkane EMRs to CO observed during ARCTAS, with the strongest correlation between the C_2–C_4 alkanes and slightly higher variability for the C_5 alkanes, primarily due to lower mixing ratios and measurement uncertainties. In general, these correlations are linear and are attributed to correlated emissions rather than chemical loss.

References

Alvarado, M. J., Logan, J. A., Mao, J., Apel, E., Riemer, D., Blake, D., Cohen, R. C., Min, K.-E., Perring, A. E., Browne, E. C., Wooldridge, P. J., Diskin, G. S., Sachse, G. W., Fuelberg, H., Sessions, W. R., Harrigan, D. L., Huey, G., Liao, J., Case-Hanks, A., Jimenez, J. L., Cubison, M. J., Vay, S. A., Weinheimer, A. J., Knapp, D. J., Montzka, D. D., Flocke, F. M., Pollack, I. B., Wennberg, P. O., Kurten, A., Crounse, J., Clair, J. M. St., Wisthaler, A., Mikoviny, T., Yantosca, R. M., Carouge, C. C., and Le Sager, P.: Nitrogen oxides and PAN in plumes from boreal fires during ARCTAS-B and their impact on ozone: an integrated analysis of aircraft and satellite observations, Atmos. Chem. Phys., 10, 9739–9760, doi:10.5194/acp-10-9739-2010, 2010.

Andreae, M. O. and Merlet, P.: Emission of trace gases and aerosols from biomass burning, Global Biogeochem. Cy., 15, 955–966, doi:10.1029/2000GB001382, 2001.

Apel, E. C., Calvert, J. G., and Fehsenfeld, F. C.: The Nonmethane Hydrocarbon Intercomparison Experiment (NOMHICE): tasks 1 and 2, J. Geophys. Res., 99, D8, 16651–16664, doi:10.1029/94JD00086, 1994.

Apel, E. C., Calvert, J. G., Gilpin, T. M., Fehsenfeld, F. C., Parrish, D. D., and Lonneman, W. A.: The Nonmethane Hydrocarbon Intercomparison Experiment (NOMHICE): task 3, J. Geophys. Res., 104, D8, 16651–16664, doi:10.1029/1999JD900793, 1999.

Apel, E. C., Hills, A. J., Lueb, R., Zindel, S., Eisele, S., and Riemer, D. D.: A fast-GC/MS system to measure C_2 to C_4 carbonyls and methanol aboard aircraft, J. Geophys. Res., 108, 8794, doi:10.1029/2002JD003199, 2003.

Apel, E. C., Emmons, L. K., Karl, T., Flocke, F., Hills, A. J., Madronich, S., Lee-Taylor, J., Fried, A., Weibring, P., Walega, J., Richter, D., Tie, X., Mauldin, L., Campos, T., Weinheimer, A., Knapp, D., Sive, B., Kleinman, L., Springston, S., Zaveri, R., Ortega, J., Voss, P., Blake, D., Baker, A., Warneke, C., Welsh-Bon, D., de Gouw, J., Zheng, J., Zhang, R., Rudolph, J., Junkermann, W., and Riemer, D. D.: Chemical evolution of volatile organic

ARCTAS VOCs: biomass burning enhancements

R. S. Hornbrook et al.

Title Page

Abstract	Introduction
Conclusions	References
Tables	Figures

|◄ | ►|
| ◄ | ► |

Back | Close

Full Screen / Esc

Printer-friendly Version

Interactive Discussion

compounds in the outflow of the Mexico City Metropolitan area, Atmos. Chem. Phys., 10, 2353–2375, doi:10.5194/acp-10-2353-2010, 2010.

Atkinson, R.: Atmospheric chemistry of VOCs and NO_x, Atmos. Environ., 34, 2063–2101, doi:10.1016/S1352-2310(99)00460-4, 2000.

Atkinson, R. and Arey, J.: Atmospheric degradation of volatile organic compounds, Chem. Rev., 103, 4605–4638, doi:10.1021/cr0206420, 2003.

Blake, N. J., Blake, D. R., Sive, B. C., Chen, T. Y., Rowland, F. S., Collins, J. E., Sachse, G. W., and Anderson, B. E.: Biomass burning emissions and vertical distribution of atmospheric methyl halides and other reduced carbon gases in the South Atlantic region, J. Geophys. Res., 101(D19), 24151–24164, doi:10.1029/96JD00561, 1996.

Burling, I. R., Yokelson, R. J., Griffith, D. W. T., Johnson, T. J., Veres, P., Roberts, J. M., Warneke, C., Urbanski, S. P., Reardon, J., Weise, D. R., Hao, W. M., and de Gouw, J.: Laboratory measurements of trace gas emissions from biomass burning of fuel types from the southeastern and southwestern United States, Atmos. Chem. Phys., 10, 11115–11130, doi:10.5194/acp-10-11115-2010, 2010.

Christian, T. J., Kleiss, B., Yokelson, R. J., Holzinger, R., Crutzen, P. J., Hao, W. M., Saharjo, B. H., and Ward, D. E.: Comprehensive laboratory measurements of biomass-burning emissions: 1. Emissions from Indonesian, African, and other fuels, J. Geophys. Res., 108, 4719, doi:10.1029/2003JD003704, 2003.

Christian, T. J., Kleiss, B., Yokelson, R. J., Holzinger, R., Crutzen, P. J., Hao, W. M., Shirai, T., and Blake, D. R.: Comprehensive laboratory measurements of biomass-burning emissions: 2. First intercomparison of open-path FTIR, PTR-MS, and GC-MS/FID/ECD, J. Geophys. Res., 109, D02311, doi:10.1029/2003JD003874, 2004.

Christian, T. J., Yokelson, R. J., Carvalho Jr., J. A., Griffith, D. W. T., Alvarado, E. C., Santos, J. C., Neto, T. G. S., Gurgel Veras, C. A., and Hao, W. M.: The tropical forest and fire emissions experiment: trace gases emitted by smoldering logs and dung from deforestation and pasture fires in Brazil, J. Geophys. Res., 112, D18308, doi:10.1029/2006JD008147, 2007.

Ciccioli, P., Brancaleoni, E., Frattoni, M., Cecinato, A., and Pinciarelli, L.: Determination of volatile organic compounds (VOC) emitted from biomass burning of Mediterranean vegetation species by GC-MS, Anal. Lett., 34, 937–955, doi:10.1081/AL-100103604, 2001.

Colarco, P. R., Schoeberl, M. R., Doddridge, B. G., Marufu, L. T., Torres, O., and Welton, E. J.: Transport of smoke from Canadian forest fires to the surface near Washington

ARCTAS VOCs: biomass burning enhancements

R. S. Hornbrook et al.

Title Page	
Abstract	Introduction
Conclusions	References
Tables	Figures

|◄ | ►|

◄ | ►

Back | Close

Full Screen / Esc

Printer-friendly Version

Interactive Discussion

DC: injection height, entrainment, and optical properties, J. Geophys. Res., 109, D06203, doi:10.1029/2003JD004248, 2004.

Colman, J. J., Swanson, A. L., Meinardi, S., Sive, B. C., Blake, D. R., and Rowland, F. S.: Description of the analysis of a wide range of volatile organic compounds in whole air samples collected during PEM-Tropics A and B, Anal. Chem., 73, 3723–3731, doi:10.1021/ac010027g, 2001.

Crounse, J. D., McKinney, K. A., Kwan, A. J., and Wennberg, P. O.: Measurement of gas-phase hydroperoxides by chemical ionization mass spectrometry, Anal. Chem., 78, 6726–6732, doi:10.1021/ac0604235, 2006.

Crounse, J. D., DeCarlo, P. F., Blake, D. R., Emmons, L. K., Campos, T. L., Apel, E. C., Clarke, A. D., Weinheimer, A. J., McCabe, D. C., Yokelson, R. J., Jimenez, J. L., and Wennberg, P. O.: Biomass burning and urban air pollution over the Central Mexican Plateau, Atmos. Chem. Phys., 9, 4929–4944, doi:10.5194/acp-9-4929-2009, 2009.

Damoah, R., Spichtinger, N., Forster, C., James, P., Mattis, I., Wandinger, U., Beirle, S., Wagner, T., and Stohl, A.: Around the world in 17 days – hemispheric-scale transport of forest fire smoke from Russia in May 2003, Atmos. Chem. Phys., 4, 1311–1321, doi:10.5194/acp-4-1311-2004, 2004.

Duck, T. J., Firanski, B. J., Millet, D. B., Goldstein, A. H., Allan, J., Holzinger, R., Worsnop, D. R., White, A. B., Stohl, A., Dickinson, C. S., and van Donkelaar, A.: Transport of forest fire emissions from Alaska and the Yukon Territory to Nova Scotia during summer 2004, J. Geophys. Res., 112, D10S44, doi:10.1029/2006JD007716, 2007.

Fuelberg, H. E., Harrigan, D. L., and Sessions, W.: A meteorological overview of the ARCTAS 2008 mission, Atmos. Chem. Phys., 10, 817–842, doi:10.5194/acp-10-817-2010, 2010.

Fisher, J. A., Jacob, D. J., Purdy, M. T., Kopacz, M., Le Sager, P., Carouge, C., Holmes, C. D., Yantosca, R. M., Batchelor, R. L., Strong, K., Diskin, G. S., Fuelberg, H. E., Holloway, J. S., Hyer, E. J., McMillan, W. W., Warner, J., Streets, D. G., Zhang, Q., Wang, Y., and Wu, S.: Source attribution and interannual variability of Arctic pollution in spring constrained by aircraft (ARCTAS, ARCPAC) and satellite (AIRS) observations of carbon monoxide, Atmos. Chem. Phys., 10, 977–996, doi:10.5194/acp-10-977-2010, 2010.

Friedli, H. R., Atlas, E., Stroud, V. R., Giovanni, L., Campos, T., and Radke, L. F.: Volatile organic trace gases emitted from North American wildfires, Global Biogeochem. Cy., 15(02), 435–452, doi:10.1029/2000GB001328, 2001.

Fromm, M., Alfred, J., Hoppel, K., Hornstein, J., Bevilacqua, R., Shettle, E., Servranckx, R.,

Title Page

Abstract	Introduction
Conclusions	References
Tables	Figures

| ◄◄ | ►► |
| ◄ | ► |

| Back | Close |

Full Screen / Esc

Printer-friendly Version

Interactive Discussion

Li, Z. Q., and Stocks, B.: Observations of boreal forest fire smoke in the stratosphere by POAM III, SAGE II, and lidar in 1998, Geophys. Res. Lett., 27, 1407–1410, doi:10.1029/1999GL011200, 2000.

de Gouw, J. A. and Warneke, C.: Measurements of volatile organic compounds in the earth's atmosphere using proton-transfer-reaction mass spectrometry, Mass Spectrom. Rev., 26, 223–257, doi:10.1002/mas.20119, 2007.

de Gouw, J. A., Warneke, C., Parrish, D. D., Holloway, J. S., Trainer, M., and Fehsenfeld, F. C.: Emission sources and ocean uptake of acetonitrile (CH_3CN) in the atmosphere, J. Geophys. Res., 108, 4329, doi:10.1029/2002JD002897, 2003.

de Gouw, J. A., Middlebrook, A. M., Warneke, C., Goldan, P. D., Kuster, W. C., Roberts, J. M., Fehsenfeld, F. C., Worsnop, D. R., Canagaratna, M. R., Pszenny, A. A. P., Keene, W. C., Marchewka, M., Bertman, S. B., and Bates, T. S.: Budget of organic carbon in a polluted atmosphere: Results from the New England Air Quality Study in 2002, J. Geophys. Res., 110, D16305, doi:10.1029/2004JD005623, 2005.

de Gouw, J. A., Warneke, C., Stohl, A., Wollny, A. G., Brock, C. A., Cooper, O. R., Holloway, J. S., Trainer, M., Fehsenfeld, F. C., Atlas, E. L., Donnelly, S. G., Stroud, V., and Lueb, A.: Volatile organic compounds composition of merged and aged forest fire plumes from Alaska and Western Canada, J. Geophys. Res., 111, D10303, doi:10.1029/2005JD006175, 2006.

de Gouw, J. A., Welsh-Bon, D., Warneke, C., Kuster, W. C., Alexander, L., Baker, A. K., Beyersdorf, A. J., Blake, D. R., Canagaratna, M., Celada, A. T., Huey, L. G., Junkermann, W., Onasch, T. B., Salcido, A., Sjostedt, S. J., Sullivan, A. P., Tanner, D. J., Vargas, O., Weber, R. J., Worsnop, D. R., Yu, X. Y., and Zaveri, R.: Emission and chemistry of organic carbon in the gas and aerosol phase at a sub-urban site near Mexico City in March 2006 during the MILAGRO study, Atmos. Chem. Phys., 9, 3425–3442, doi:10.5194/acp-9-3425-2009, 2009.

Holzinger, R., Williams, J., Salisbury, G., Klüpfel, T., de Reus, M., Traub, M., Crutzen, P. J., and Lelieveld, J.: Oxygenated compounds in aged biomass burning plumes over the Eastern Mediterranean: evidence for strong secondary production of methanol and acetone, Atmos. Chem. Phys., 5, 39–46, doi:10.5194/acp-5-39-2005, 2005.

Hornbrook, R. S., Blake, D., Crounse, J. D., Diskin, G. S., Flocke, F., Fuelberg, H. E., Knapp, D. J., Mauldin III, R. L., Mikoviny, T., Montzka, D. D., Pollack, I. B., St. Clair, J. M., Vay, S. A., Weinheimer, A. J., Wennberg, P. O., Wisthaler, A., Hills, A., Riemer, D. D., and

Title Page

Abstract | Introduction

Conclusions | References

Tables | Figures

◀ | ▶

◀ | ▶

Back | Close

Full Screen / Esc

Printer-friendly Version

Interactive Discussion

Apel, E. C.: Observations of volatile organic compounds during ARCTAS – Part 2: Contrasting anthropogenic and biomass burning emissions, in preparation, 2011.

Jacob, D. J., Crawford, J. H., Maring, H., Clarke, A. D., Jacob, D. J., Crawford, J. H., Maring, H., Clarke, A. D., Dibb, J. E., Emmons, L. K., Ferrare, R. A., Hostetler, C. A., Russell, P. B., Singh, H. B., Thompson, A. M., Shaw, G. E., McCauley, E., Pederson, J. R., and Fisher, J. A.: The Arctic Research of the Composition of the Troposphere from Aircraft and Satellites (ARCTAS) mission: design, execution, and first results, Atmos. Chem. Phys., 10, 5191–5212, doi:10.5194/acp-10-5191-2010, 2010.

Jost, C., Trentmann, J., Sprung, D., Andreae, M. O., McQuaid, J. B., and Barjat, H.: Trace gas chemistry in a young biomass burning plume over Namibia: observations and model simulations, J. Geophys. Res., 108, 8482, doi:10.1029/2002JD002431, 2003.

Jost, H. J., Drdla, K., Stohl, A., Pfister, L., Loewenstein, M., Lopez, J. P., Hudson, P. K., Murphy, D. M., Cziczo, D. J., Fromm, M., Bui, T. P., Dean-Day, J., Gerbig, C., Mahoney, M. J., Richard, E. C., Spichtinger, N., Pittman, J. V., Weinstock, E. M., Wilson, J. C., and Xueref, I.: In-situ observations of mid-latitude forest fire plumes deep in the stratosphere, Geophys. Res. Lett., 31, L11101, doi:10.1029/2003GL019253, 2004.

Katzenstein, A. S., Doezema, L. A., Simpson, I. J., Blake, D. R., and Rowland, F. S.: Extensive regional atmospheric hydrocarbon pollution in the Southwestern United States, P. Natl. Acad. Sci. USA, 100(21), 11975–11979, doi:10.1073/pnas.1635258100, 2003.

Levine, J. S.: Global biomass burning: a case study of the gaseous and particulate emissions released to the atmosphere during the 1997 fires in Kalimantan and Sumatra, Indonesia, in: Biomass Burning and its Inter-Relationships with the Climate System, edited by: Innes, J. L., Beniston, M., and Verstraete, M. M., Kluwar Academic Publishers, Boston, 15–31, 2000.

Li, Q. B., Jacob, D. J., Bey, I., Yantosca, R. M., Zhao, Y. J., Kondo, Y., and Notholt, J.: Atmospheric hydrogen cyanide (HCN): biomass burning source, ocean sink?, Geophys. Res. Lett., 27, 357–360, doi:10.1029/1999GL010935, 2000.

Lobert, J. M., Scharffe, D. H., Hao, W. M., and Crutzen, P. J.: Importance of biomass burning in the atmospheric budgets of nitrogen-containing gases, Nature, 346, 552–554, doi:10.1038/346552a0, 1990.

Madronich, S.: Chemical evolution of gaseous pollutants downwind of tropical megacities: Mexico City case study, Atmos. Environ., 40, 6012–6018, doi:10.1016/j.atmosenv.2005.08.047, 2006.

Madronich, S. and Calvert, J. G.: Permutation reactions of organic peroxy radicals in the tropo-

sphere, J. Geophys. Res., 95(D5), 5697–5715, doi:10.1029/JD095iD05p05697, 1990.

Madronich, S. and Flocke, S: The role of solar radiation in atmospheric chemistry, in: Handbook of Environmental Chemistry, edited by: Boule, P., Springer-Verlag, Heidelberg, Germany, 1–26, 1999.

5 Monks, P. S., Granier, C., Fuzzi, S., Stohl, A., Williams, M. L., Akimoto, H., Amann, M., Baklanov, A., Baltensperger, U., Bey, I., Blake, N., Blake, R. S., Carslaw, K., Cooper, O. R., Dentener, F., Fowler, D., Fragkou, E., Frost, G. J., Generoso, S., Ginoux, P., Grewe, V., Guenther, A., Hansson, H. C., Henne, S., Hjorth, J., Hofzumahaus, A., Huntrieser, H., Isaksen, I. S. A., Jenkin, M. E., Kaiser, J., Kanakidou, M., Klimont, Z., Kulmala, M.,
10 Laj, P., Lawrence, M. G., Lee, J. D., Liousse, C., Maione, M., McFiggans, G., Metzger, A., Mieville, A., Moussiopoulos, N., Orlando, J. J., O'Dowd, C. D., Palmer, P. I., Parrish, D. D., Petzold, A., Platt, U., Poeschl, U., Prevot, A. S. H., Reeves, C. E., Reimann, S., Rudich, Y., Sellegri, K., Steinbrecher, R., Simpson, D., ten Brink, H., Theloke, J., van der Werf, G. R., Vautard, R., Vestreng, V., Vlachokostas, C., and von Glasow, R.: Atmospheric
15 composition change – global and regional air quality, Atmos. Environ., 43, 5268–5350, doi:10.1016/j.atmosenv.2009.08.021, 2009.

Morris, G. A., Hersey, S., Thompson, A. M., Pawson, S., Nielsen, J. E., Colarco, P. R., McMillan, W. W., Stohl, A., Turquety, S., Warner, J., Johnson, B. J., Kucsera, T. L., Larko, D. E., Oltmans, S. J., and Witte, J. C.: Alaskan and Canadian forest fires exacerbate ozone
20 pollution over Houston, Texas, on 19 and 20 July 2004, J. Geophy. Res., 111, D24S03, doi:10.1029/2006JD007090, 2006.

Raber, W. H. and Moortgat, G. K.: Photooxidation of selected carbonyl compounds in air: methyl ethyl keton, methyl vinyl ketone, methacrolein and methylglyoxal, in: Progress and Problems in Atmospheric Chemistry, edited by: Barker, J. R., World Scientific, New Jersey,
25 318–373, 1995.

Sachse, G. W., Harriss, R. C., Fishman, J., Hill, G. F., and Cahoon, D. R.: Carbon monoxide over the Amazon Basin during the 1985 dry season, J. Geophys. Res., 93, 1422–1430, doi:10.1029/JD093iD02p01422, 1988.

Shim, C., Wang, Y., Singh, H. B., Blake, D. R., and Guenther, A. B.: Source characteristics
30 of oxygenated volatile organic compounds and hydrogen cyanide, J. Geophys. Res., 112, D10305, doi:10.1029/2006JD007543, 2007.

Simpson, I. J., Blake, N. J., Barletta, B., Diskin, G. S., Fuelberg, H. E., Gorham, K., Huey, L. G., Meinardi, S., Rowland, F. S., Vay, S. A., Weinheimer, A. J., Yang, M., and Blake, D. R.: Char-

ARCTAS VOCs: biomass burning enhancements

R. S. Hornbrook et al.

Title Page

Abstract	Introduction
Conclusions	References
Tables	Figures

◄◄ ►►

◄ ►

Back Close

Full Screen / Esc

Printer-friendly Version

Interactive Discussion

acterization of trace gases measured over Alberta oil sands mining operations: 76 speciated C_2–C_{10} volatile organic compounds (VOCs), CO_2, CH_4, CO, NO, NO_2, NO_y, O_3 and SO_2, Atmos. Chem. Phys., 10, 11931–11954, doi:10.5194/acp-10-11931-2010, 2010.

Singh, H. B., Ohara, D., Herlth, D., Sachse, W., Blake, D. R., Bradshaw, J. D., Kanakidou, M., and Crutzen, P. J.: Acetone in the atmosphere – distribution, sources, and sinks, J. Geophys. Res., 99, 1805–1819, doi:10.1029/93JD00764, 1994.

Sinha, P., Hobbs, P. V., Yokelson, R. J., Bertschi, I. T., Blake, D. R., Simpson, I. J., Gao, S., Kirchstetter, T. W., and Novakov, T.: Emissions of trace gases and particles from savanna fires in Southern Africa, J. Geophys. Res., 108, 8487, doi:10.1029/2002JD002325, 2003.

Sinha, P., Hobbs, P. V., Yokelson, R. J., Blake, D. R., Gao, S., and Kirchstetter, T. W.: Emissions from miombo woodland and dambo grassland savanna fires, J. Geophys. Res., 109, D11305, doi:10.1029/2004JD004521, 2004.

Tilmes, S., Emmons, L. K., Law, K. S., Ancellet, G., Schlager, H., Paris, J.-D., Fuelberg, H. E., Streets, D. G., Wiedinmyer, C., Diskin, G. S., Kondo, Y., Holloway, J., Schwartz, J. P., Spackman, J. R., Campos, T., Nédélec, P., and Panchenko, M. V.: Source contributions to Northern Hemisphere CO and black carbon during spring and summer 2008 from POLARCAT and START08/preHIPPO observations and MOZART-4, Atmos. Chem. Phys. Discuss., 11, 5935–5983, doi:10.5194/acpd-11-5935-2011, 2011.

Val Martin, M., Logan, J. A., Kahn, R. A., Leung, F.-Y., Nelson, D. L., and Diner, D. J.: Smoke injection heights from fires in North America: analysis of 5 years of satellite observations, Atmos. Chem. Phys., 10, 1491–1510, doi:10.5194/acp-10-1491-2010, 2010.

Vay, S. A., Woo, J.-H., Anderson, B. E., Thornhill, K. L., Blake, D. R., Westberg, D. J., Kiley, C. M., Avery, M. A., Sachse, G. W., Streets, D. G., Tsutsumi, Y., and Nolf, S. R.: Influence of regional-scale anthropogenic emissions on CO_2 distributions over the Western North Pacific, J. Geophys. Res., 108(D20), 8801, doi:10.1029/2002JD003094, 2003.

Vivchar, A. V., Moiseenko, K. B., and Pankratova, N. V.: Estimates of carbon monoxide emissions from wildfires in Northern Eurasia for airquality assessment and climate modeling, Izv. Atmos. Oceanic Phys., 46, 281–293, doi:10.1134/S0001433810030023, 2010.

Ward, D. E. and Radke, L. F.: Emission measurements from vegetation fires: a comparative evaluation of methods and results, in: Fire in the Environment: the Ecological Atmospheric, and Climatic Importance of Vegetation Fires, edited by: Crutzen, P. J. and Goldammer, J. G., John Wiley and Sons, New York, 53–76, 1993.

Warneke, C., McKeen, S. A., de Gouw, J. A., Goldan, P. D., Kuster, W. C., Holloway, J. S.,

ARCTAS VOCs: biomass burning enhancements

R. S. Hornbrook et al.

Title Page

Abstract	Introduction
Conclusions	References
Tables	Figures

◄◄	►►
◄	►
Back	Close

Full Screen / Esc

Printer-friendly Version

Interactive Discussion

Williams, E. J., Lerner, B. M., Parrish, D. D., Trainer, M., Fehsenfeld, F. C., Kato, S., Atlas, E. L., Baker, A., and Blake, D. R.: Determination of urban volatile organic compound emission ratios and comparison with an emissions database, J. Geophys. Res., 112, D10S47, doi:10.1029/2006JD007930, 2007.

Wiedinmyer, C., Akagi, S. K., Yokelson, R. J., Emmons, L. K., Al-Saadi, J. A., Orlando, J. J., and Soja, A. J.: The Fire INventory from NCAR (FINN) – a high resolution global model to estimate the emissions from open burning, Geosci. Model Dev. Discuss., 3, 2439-2476, doi:10.5194/gmdd-3-2439-2010, 2010.

Yokelson, R. J., Karl, T., Artaxo, P., Blake, D. R., Christian, T. J., Griffith, D. W. T., Guenther, A., and Hao, W. M.: The Tropical Forest and Fire Emissions Experiment: overview and airborne fire emission factor measurements, Atmos. Chem. Phys., 7, 5175–5196, doi:10.5194/acp-7-5175-2007, 2007a.

Yokelson, R. J., Urbanski, S. P., Atlas, E. L., Toohey, D. W., Alvarado, E. C., Crounse, J. D., Wennberg, P. O., Fisher, M. E., Wold, C. E., Campos, T. L., Adachi, K., Buseck, P. R., and Hao, W. M.: Emissions from forest fires near Mexico City, Atmos. Chem. Phys., 7, 5569–5584, doi:10.5194/acp-7-5569-2007, 2007b.

Yokelson, R. J., Christian, T. J., Karl, T. G., and Guenther, A.: The tropical forest and fire emissions experiment: laboratory fire measurements and synthesis of campaign data, Atmos. Chem. Phys., 8, 3509–3527, doi:10.5194/acp-8-3509-2008, 2008.

Yokelson, R. J., Crounse, J. D., DeCarlo, P. F., Karl, T., Urbanski, S., Atlas, E., Campos, T., Shinozuka, Y., Kapustin, V., Clarke, A. D., Weinheimer, A., Knapp, D. J., Montzka, D. D., Holloway, J., Weibring, P., Flocke, F., Zheng, W., Toohey, D., Wennberg, P. O., Wiedinmyer, C., Mauldin, L., Fried, A., Richter, D., Walega, J., Jimenez, J. L., Adachi, K., Buseck, P. R., Hall, S. R., and Shetter, R.: Emissions from biomass burning in the Yucatan, Atmos. Chem. Phys., 9, 5785–5812, doi:10.5194/acp-9-5785-2009, 2009.

Yuan, B., Liu, Y., Shao, M., Lu, S., and Streets, D. G.: Biomass burning contributions to ambient VOCs species at a receptor site in the Pearl River Delta (PRD), China, Environ. Sci. Technol., 44, 4577–4582, doi:10.1021/es1003389, 2010.

Title Page

Abstract | Introduction

Conclusions | References

Tables | Figures

|◄ | ►|

◄ | ►

Back | Close

Full Screen / Esc

Printer-friendly Version

Interactive Discussion

Table 1. Summary of biomass burning plume encounters.

Plume group	Flight date	Plume interception times (UTC)[a]	Biomass burning plume origin	Plume age, days[a]	Modified combustion efficiency[b]
1	12 Apr	16:15–16:24; 16:39–16:58; 17:07–17:14	Asia	7	0.983 ± 0.004
2	12 Apr	17:40–18:00	Asia	5	0.97 ± 0.01
3	12 Apr	19:05–19:18; 20:04–20:12	Asia	6	0.98 ± 0.01
4	12 Apr	21:52–23:00	Asia	7	0.986 ± 0.007
5	16 Apr	20:16–20:27; 22:57–23:08; 23:20–23:39; 00:02–00:45; 00:56–01:00; 01:02–01:25; 01:46–01:50; 02:05–02:11	Siberia	7	0.983 ± 0.006
6	16 Apr	22:33–22:43	Mixed AK/Siberia	4.5	0.987 ± 0.009
7	17 Apr	20:22–20:27; 21:04–21:21	Asia	6	0.98 ± 0.02
8	17 Apr	22:05–22:20	Mixed AK/Siberia	8	0.98 ± 0.03
9	17 Apr	23:40–23:44; 00:53–01:08; 01:13–01:45; 02:00–02:10;	Western Asia	7.5	1.00 ± 0.01
10	17 Apr	03:56–04:02; 04:53–05:04; 05:22–05:36	Southern Asia	7	0.99 ± 0.03
11	19 Apr	20:10–20:41; 20:52–21:13	East Asia	4	0.962 ± 0.005
12	18 Jun	18:27–18:30; 18:38–18:41	California	1	0.93 ± 0.02
13	20 Jun	19:52–19:54; 21:35–21:40	California	0.2	0.93 ± 0.03
14	20 Jun	00:01–00:02; 00:19–00:30	California	0.2	0.917 ± 0.004
15	22 Jun	18:20–18:28; 19:41–19:48	Asia	7	0.98 ± 0.04
16	22 Jun	21:08–21:12; 21:23–21:44	California	0.1	1.0 ± 0.1
17	24 Jun	22:12–22:31	California	1.5	0.95 ± 0.04
18	26 Jun	14:32–14:35; 15:34–16:17; 16:39–16:57	California	1	0.92 ± 0.01
19	29 Jun	16:04–16:11; 21:22–21:49	Siberia	7.5	1.03 ± 0.02
20	29 Jun	18:11–19:22	Yukon	1	0.99 ± 0.06
21	29 Jun	21:56–22:22; 22:31	Saskatchewan	0.1	0.93 ± 0.01
22	1 Jul	20:15–22:00	Saskatchewan	0.1	0.930 ± 0.005
23	1 Jul	22:01–22:23; 22:29–22:30; 22:33–23:58; 00:15–00:20	Saskatchewan	0.3	0.892 ± 0.009
24	1 Jul	01:43–02:16; 02:19–02:49	Saskatchewan	0.1	0.87 ± 0.01
25	4 Jul	18:20–18:28	Saskatchewan	0.1	0.91 ± 0.05
26	4 Jul	18:45–18:51; 19:26–19:45; 20:23–20:37	California	4	1.0 ± 0.1
27	4 Jul	19:00–19:25; 22:26–22:52; 23:56–00:07; 00:26–00:56; 01:16–01:33	Saskatchewan	0.5	1.01 ± 0.03
28	4 Jul	19:52–20:22	Saskatchewan	0.1	1.01 ± 0.01
29	4 Jul	20:54–21:29; 22:12–22:19	Mixed Sask./Calif.	1	0.97 ± 0.03
30	4 Jul	01:58–02:32	Saskatchewan	1	0.9 ± 0.1
31	5 Jul	20:41–20:59	Mixed Sask./Calif.	3	0.97 ± 0.04
32	5 Jul	21:06–21:22	Saskatchewan	2	1.03 ± 0.03
33	5 Jul	23:37–23:58; 01:03–01:15; 01:19–01:37; 01:43–01:54	California	5	1.02 ± 0.01
34	5 Jul	02:05–02:30	Mixed Sask./Calif.	3	1.0 ± 0.1
35	8 Jul	09:19–09:31; 09:39–10:28	Asia	5	1.01 ± 0.06
36	8 Jul	12:48–13:04	Asia	8	1.01 ± 0.04
37	8 Jul	14:59–16:08	Asia	5	1.0 ± 0.1
38	13 Jul	18:31–18:38	East Asia	5	1.04 ± 0.02
39	13 Jul	19:34–20:26; 20:32–21:01	California	0.5	0.97 ± 0.01
40	13 Jul	21:02–21:44	California	0.5	0.99 ± 0.05

[a] Estimated based on back-trajectories, flight tracks, and fire data. Times between 00:00 and 06:00 UTC occurred on the following date after UTC midnight for flights that began the previous UTC day.

[b] Uncertainty determined from the standard error in the slope of a linear fit of a plot of CO vs. CO_2 using data from the 1-s merge.

Title Page

Abstract | Introduction

Conclusions | References

Tables | Figures

◀◀ | ▶▶

◀ | ▶

Back | Close

Full Screen / Esc

Printer-friendly Version

Interactive Discussion

Table 2. Normalized excess mixing ratios against CO (pptv ppbv^{-1}) for selected VOCs in individual biomass burning plume groups.

Plume group	HCN[a] CIMS	Acetonitrile		Acetone			Methanol			Ethanol		Acetaldehyde	
		TOGA	PTR-MS	TOGA	PTR-MS	WAS	TOGA	PTR-MS	WAS	TOGA	WAS	TOGA	PTR-MS
1	8.5±1.0				4.8±0.7			10±1					1.1±0.2
2	4.0±0.8	0.7±0.01		8±1	6.4±0.4	7±1	17±3	11.3±0.7					0.9±0.1
3	8.3±1.3	1.2±0.3		7±2				13±1					1.1±0.1
4				8±1									
5	6.6±0.5	1.7±0.1	1.5±0.1	9.9±0.9	7.0±0.4	12±1	20±2	14.8±0.6					1.7±0.1
6	6.7±0.7	1.3±0.5	0.8±0.2	12±2	8±1		18±4	14±1					0.8±0.2
7		1.4±0.2		6±1	9±4		10±3	16±7					
8	9±2												
9	3.3±0.3			8±1	4.3±0.4			5.8±0.5					
10				9±2	9±1	14±3	17±2	13±2	18±5				1.5±0.1
11	9.5±0.4	1.3±0.1	1.92±0.05	5.5±0.6	7.5±0.2		18±1	16.1±0.3	12±1	0.6±0.1			0.88±0.06
12	3.7±0.2	1.3±0.1	2.6±0.1	3.1±0.5	4.5±0.2	4.7±0.7	19±2	15.8±0.5	18.3±0.8	0.5±0.3	0.6±0.1	4.5±0.7	5.8±0.5
13		1.5±0.2	2.5±0.3	10±2	10±1		54±9	38±4				22±4	22±2
14		1.4±0.1	1.6±0.1	2.6±0.6	3.3±0.3		10±1	10.8±0.9				3.7±0.4	3.3±0.6
15	5.5±0.8		0.6±0.2										
16	1.8±0.1	0.61±0.06	1.13±0.08	2.6±0.4	3.8±0.3		14.6±0.8	16±1				3.3±0.3	5.2±0.2
17			2.1±0.2				19±5	13±2				1.7±0.6	
18	2.38±0.05	0.66±0.04	1.47±0.03	3.7±0.2	4.7±0.2	2.3±0.2	16.6±0.7	18.2±0.6	11±1	1.2±0.2	0.48±0.08	9.4±0.5	8.0±0.3
19	9.5±0.5	1.9±0.3	1.50±0.06	15±2	13.2±0.8	7.2±1.6	41±4	22±1					
20	10.6±0.7	2.1±0.2	1.6±0.1	5.7±0.8	6.4±0.5							4.8±0.7	
21	3.7±0.8		1.60±0.08		3.1±0.2	1.5±0.2		8.1±0.8	8±1				3.7±0.6
22	6.9±0.3	1.6±0.2	1.9±0.2	11±1	14±1		25±6	24±4					
23	9.4±0.2	2.5±0.2	2.31±0.05	3.1±0.2	3.1±0.1	1.3±0.1	12.2±0.9	12.0±0.2	8.6±0.8			7.4±0.6	5.4±0.2
24	9.4±0.2	1.5±0.1	1.63±0.03	2.1±0.2	2.7±0.1	1.0±0.1	8.3±0.7	10.7±0.3	7.0±0.9	0.38±0.06		4.4±0.4	4.6±0.2
25	4.1±0.5	1.1±0.2	1.36±0.08	1.7±0.7	2.6±0.3		5±3	7±2	1.5±0.6	3±1		3.4±0.7	3.1±0.3
26	3.3±0.5	1.6±0.3	1.3±0.1										3.5±0.4
27	15.1±1.0		1.5±0.1									3.1±0.2	
28	5.4±0.2	1.4±0.1	1.8±0.3	13±2	12±1		42±6	51±5		3.6±0.8			4.5±0.7
29	5.5±0.4	1.7±0.2	1.64±0.09	3.8±0.5	4.5±0.3	1.9±0.3	11±2	14±1				8.0±0.9	6.3±0.4
30	8.6±0.4	2.0±0.4	2.35±0.08	4.4±0.4	3.7±0.1	1.6±0.2	6.9±0.7		13±2	0.25±0.04	0.38±0.08	12±1	
31	6.6±0.3	1.4±0.2	1.6±0.1		3.7±0.7							2.2±0.3	
32	5.7±0.4	2.2±0.3	2.0±0.2	9±2	10±1		35±7	51±5	41±12	1.9±0.6		2.9±0.6	4.0±0.5
33	7.0±0.9	1.9±0.2	1.7±0.1					26±3					4.2±0.8
34		3.0±0.7	2.4±0.6					34±10					
35	13.8±0.4	1.8±0.1	1.77±0.05	6.6±0.9	7.5±0.5		22±1	15.0±0.5	9±1	0.48±0.05			
36	14.9±1.0				4.8±0.7			10±1					
37		1.2±0.2		16±1	11.6±0.8								
38	12.6±1.2		1.3±0.4		11.6±0.7			10±1	6.7±0.7				
39	1.56±0.09	0.86±0.06	1.22±0.03	8±1	9.6±0.8	6.6±0.5	17±2	25±2	20±2	4.5±0.5	2.6±0.2	4.1±0.4	5.0±0.3
40	1.7±0.1		1.1±0.1	11±2	14±1	11±1							

[a] Uncertainties are the standard error in the slope of the plot of VOC X against CO.

Table 2. Continued.

Plume group	MVK + methacrolein (MAC) TOGA MVK	TOGA MAC	TOGA	WAS	WAS MAC	MEK TOGA	MEK WAS	Ethane WAS	Propane WAS	Isobutane TOGA	Isobutane WAS	Butane TOGA	Butane WAS	Isopentane TOGA	Isopentane WAS
1								6.6±0.6	2.8±0.3	0.45±0.05	0.38±0.05	0.72±0.07	0.70±0.08	0.20±0.02	
2								5.8±0.3	2.23±0.08	0.33±0.02	0.36±0.01	0.42±0.04	0.51±0.02	0.186±0.009	0.20±0.02
3								6±1		0.6±0.1		1.0±0.2		0.29±0.08	
4															
5								8.9±0.5	2.9±0.3	0.40±0.04		0.74±0.07		0.22±0.02	0.22±0.02
6						1.2±0.2		7±2		0.7±0.1		1.2±0.3	1.5±0.5	0.29±0.10	
7										0.5±0.1		1.0±0.3		0.23±0.06	
8															
9								8±1							
10						1.1±0.1		12±1	3.8±0.7		0.5±0.1		0.9±0.2		0.29±0.07
11						0.80±0.06		6.8±0.7	1.7±0.2		0.15±0.02		0.35±0.04		
12				0.5±0.2	0.27±0.09	0.66±0.06	0.17±0.02	6.3±0.5	1.4±0.1	0.070±0.009	0.07±0.01	0.25±0.03	0.26±0.02	0.03±0.02	0.028±0.009
13			2.5±0.05			2.2±0.3						0.4±0.1			
14			0.27±0.08			0.45±0.05				0.050±0.007		0.17±0.2		0.021±0.004	
15								3.1±0.9	1.4±0.3						
16	0.9±0.2	0.7±0.1				0.44±0.03				0.051±0.005		0.14±0.01			
17						0.8±0.2									
18	0.31±0.05	0.29±0.05	1.23±0.06	0.50±0.04	0.40±0.04	0.65±0.03	0.54±0.03	6.7±0.3	1.54±0.07	0.097±0.006	0.095±0.005	0.35±0.01	0.34±0.01	0.13±0.02	0.07±0.02
19						0.32±0.06		3.8±0.4					0.06±0.01		
20						0.48±0.04		5.6±0.8		0.076±0.008		0.30±0.03		0.032±0.005	
21			1.1±0.1			0.27±0.07	0.36±0.06	4.0±0.4	1.1±0.1		0.077±0.008		0.27±0.03	0.034±0.006	0.041±0.006
22			4.8±0.4												
23	0.36±0.04	0.17±0.02	0.75±0.04			0.47±0.03	0.35±0.03	4.4±0.3	1.28±0.08	0.092±0.006	0.087±0.005	0.35±0.02	0.35±0.02	0.052±0.004	0.086±0.008
24	0.21±0.03	0.10±0.02	0.72±0.03			0.30±0.03	0.22±0.03	3.1±0.2	0.92±0.08	0.055±0.004	0.065±0.005	0.18±0.02	0.26±0.02	0.031±0.003	0.057±0.007
25			0.71±0.04			0.4±0.1	0.4±0.1	2.7±0.7	0.7±0.02			0.25±0.06	0.18±0.06		
26								3.5±0.4							
27	2.7±0.3	1.8±0.2	4.7±0.4			0.69±0.06				0.31±0.04		0.66±0.07			
28	6±1	3.1±0.7				2.3±0.3		19±3	17±3	2.4±0.2	2.1±0.03	5.1±0.7	5.5±0.08		1.1±0.02
29	0.53±0.10		0.9±0.1			0.56±0.06		4.5±0.5		0.07±0.01	0.07±0.01	0.25±0.03	0.24±0.03		0.033±0.008
30	0.9±0.2	0.6±0.1	1.5±0.2			0.59±0.06	0.48±0.06	6.1±0.8	1.7±0.2	0.14±0.01	0.12±0.02	0.51±0.04	0.43±0.05	0.08±0.01	0.08±0.01
31	0.6±0.1	0.52±0.09	1.1±0.1			0.37±0.07						0.35±0.09			
32	0.7±0.2	0.3±0.1	1.2±0.3			0.8±0.2		5±1	1.8±0.4			0.5±0.2	0.5±0.2	0.12±0.04	
33	0.9±0.1	0.43±0.06	1.3±0.1			0.69±0.08		6.5±0.4	2.1±0.3		0.29±0.04	0.7±0.1	0.73±0.07		0.21±0.03
34															
35						0.35±0.02		4.7±0.3	1.17±0.09	0.09±0.01	0.09±0.01	0.24±0.02	0.25±0.03	0.023±0.003	0.035±0.007
36						0.21±0.02		3±1		0.056±0.008		0.15±0.02			
37								4.6±0.5							
38								6.8±0.7	1.8±0.2						
39						0.79±0.06	0.75±0.05	6.5±0.2	2.30±0.09	0.14±0.01	0.165±0.008	0.29±0.02	0.38±0.01	0.28±0.05	0.32±0.02
40						0.7±0.1		5.1±0.6					0.7±0.1		

Title Page

Abstract | Introduction

Conclusions | References

Tables | Figures

◄◄ | ►►

◄ | ►

Back | Close

Full Screen / Esc

Printer-friendly Version

Interactive Discussion

Table 2. Continued.

Plume group	Pentane TOGA	Pentane WAS	Benzene TOGA	Benzene PTR-MS	Benzene WAS	Toluene TOGA	Toluene PTR-MS	Toluene WAS	Ethylbenzene/p,m-xylene TOGA	Ethylbenzene/p,m-xylene WAS	o-Xylene TOGA	o-Xylene WAS
1	0.15±0.02	0.14±0.02	1.2±0.2	1.4±0.1	0.9±0.1							
2	0.12±0.02	0.124±0.006	1.2±0.2	1.4±0.1	1.42±0.09		0.1±0.02					
3			1.5±0.2	1.7±0.3			0.11±0.02	0.09±0.03				
4	0.20±0.02	0.23±0.02		1.50±0.2								
5	0.29±0.05		1.18±0.09	1.50±0.05	1.90±0.07		0.17±0.02	0.36±0.03				
6	0.22±0.06		1.3±0.2	1.2±0.2	0.8±0.3		0.10±0.02					
7				1.5±0.6								
8				1.5±0.2								
9				1.35±0.08	1.2±0.1							
10		0.20±0.04		1.4±0.2	1.6±0.2			0.17±0.03				
11		0.079±0.008	0.95±0.06	1.29±0.04	1.4±0.1			0.059±0.009				
12	0.12±0.01	0.089±0.006	1.0±0.2	1.50±0.08	1.8±0.1	0.59±0.03	0.52±0.07	0.60±0.05	0.09±0.02	0.070±0.006	0.020±0.009	0.031±0.004
13			1.18±0.06	1.24±0.07		0.74±0.08	1.0±0.2		0.20±0.04		0.18±0.03	
14	0.061±0.005		1.2±0.1	1.2±0.1		0.41±0.06	0.44±0.04		0.08±0.01		0.07±0.01	
15	0.051±0.009			0.64±0.09								
16			0.99±0.07	1.33±0.07		0.53±0.04	0.50±0.06		0.039±0.009		0.012±0.002	
17			1.2±0.3	1.24±0.06	1.0±0.3	0.31±0.07						0.04±0.02
18	0.160±0.006	0.152±0.007	1.63±0.04	1.69±0.03	2.3±0.1	0.85±0.02	0.96±0.03	1.13±0.05	0.168±0.009	0.122±0.009	0.033±0.003	0.17±0.01
19			0.63±0.05	0.69±0.07	0.64±0.07							
20	0.12±0.01		1.4±0.1	1.2±0.1	1.3±0.2	0.57±0.05	0.39±0.05		0.05±0.01			
21		0.12±0.01		1.48±0.06	1.8±0.1			0.90±0.07		0.092±0.009		0.13±0.01
22												
23	0.18±0.01	0.151±0.009	1.4±0.1	1.49±0.03	1.8±0.1	0.64±0.02	0.45±0.04	0.66±0.05	0.092±0.007	0.051±0.006	0.068±0.006	
24	0.103±0.009	0.12±0.01	0.87±0.07	1.07±0.03	1.2±0.1	0.44±0.02	0.29±0.03	0.42±0.03	0.070±0.006	0.035±0.005	0.054±0.006	0.059±0.009
25	0.12±0.01	0.10±0.02	1.5±0.3	1.25±0.08	1.2±0.3	0.42±0.04	0.38±0.07	0.32±0.09	0.08±0.02	0.022±0.007	0.05±0.05	0.028±0.009
26			1.8±0.2	1.00±0.07	1.04±0.04	0.29±0.04		0.35±0.03				
27	0.24±0.02		0.9±0.1	1.4±0.1		0.61±0.05	0.18±0.02		0.019±0.003			
28	0.8±0.8	1.2±0.2	1.5±0.3		1.2±0.2		0.15±0.02					
29	0.11±0.01	0.10±0.01	1.8±0.2	1.68±0.06	1.5±0.2	0.67±0.04	0.53±0.06	0.53±0.06	0.076±0.009	0.036±0.006	0.052±0.006	
30	0.23±0.02	0.19±0.02	2.2±0.2	1.71±0.04	2.3±0.3	0.62±0.03	0.62±0.07	0.9±0.1	0.12±0.02	0.09±0.02	0.10±0.01	0.16±0.04
31	0.13±0.03		1.2±0.1	1.3±0.1		0.56±0.06	0.40±0.06		0.07±0.01		0.04±0.01	
32	0.15±0.04	0.20±0.05	1.1±0.1	1.5±0.2	1.0±0.2		0.25±0.03	0.20±0.04	0.039±0.004		0.031±0.006	
33	0.18±0.03	0.26±0.02	1.1±0.1	1.19±0.08	1.34±0.07	0.40±0.03	0.35±0.02	0.37±0.02	0.026±0.004			
34			1.4±0.2				0.4±0.1		0.06±0.01			
35	0.065±0.006	0.078±0.008	1.02±0.06	1.13±0.06	1.08±0.07		0.082±0.008					
36	0.029±0.009		0.8±0.1	0.86±0.05		0.12±0.03	0.012±0.003					
37			0.78±0.08		0.60±0.05							
38				0.61±0.06								
39	0.14±0.01	0.17±0.01	1.15±0.05	1.32±0.04	1.37±0.07	0.47±0.03	0.40±0.03	0.47±0.03	0.068±0.008			
40			0.7±0.1		0.9±0.1							

Table 3. Selected literature normalized excess mixing ratios (EMRs) and mean observed VOC EMRs by biomass burning source region during ARCTAS.[a]

Compound	Andreae[b]	Friedli[c]	Sinha[d]	de Gouw[e]	Yokelson[f]	Warneke[g]	Yuan[h]	This work[i]
HCN	0.43±0.15 (Sv) 1.5 (TF)[j] 1.4 (ET)[j]		9±3 (Sv) 6±2 (W) 9±5 (G)		12.8±9.5 (MC) 6.6±4.8 (Yu) 7.0±5.9 (TF)			8.8±3.8 (As)[k] 3.1±1.9 (CA)[k] 7.6±3.2 (Can)[k]
CH$_3$CN	1.2 (Sv) 1.2 (TF)[j] 1.2 (ET)			2.4±0.7	4.3 (Yu) 2.4±0.9 (TF)	2.6±1.3 (As) 2.4±0.7 (Can)		1.4±0.4 (As) 1.4±0.7 (CA) 1.7±0.4 (Can)
Acetone	2.1±1.5 (Sv) 2.9 (TF) 2.5±0.9 (ET)	1.70 (CA) 2.05 (ET)		6.3±5.7	6.6 (Yu) 2.7±1.0 (TF)	10±6 (As) 6±5 (Can)	6.4±2.6	9.0±3.6 (As) 6.0±3.8 (CA) 5.9±4.0 (Can)
Acetaldehyde	4.9±4.1 (Sv) 4.0 (TF) 3.0±1.0 (ET)	2.35 (CA) 2.7 (ET)		1.6±1.4	18.7 (Yu) 8.7±5.1 (TF)		3.0±1.3	1.2±0.3 (As)[l] 6.9±6.9 (CA) 5.4±3.2 (Can)
Methanol	18 (Sv) 17 (TF) 16±13 (ET)	1.80 (CA) 2.4 (ET)	15±3 (Sv) 13±1 (W) 11±4 (G)	11±6	22±11 (MC) 27±2 (Yu) 22±6 (TF)	26±14 (As) 11±5 (Can)	12.6±8.5	21±10 (As) 21±15 (CA) 18±14 (Can)
Ethanol	0.10 (Sv) 0.10 (TF) 0.10 (ET)							0.56±0.11 (As) 2.1±2.1 (CA) 1.8±1.5 (Can)
MEK	1.6 (Sv) 1.6 (TF) 1.7±1.2 (ET)	1.55 (CA) 2.60 (ET)		0.7±0.5	3.0 (Yu) 1.7±0.9 (TF)	1.4±0.8 (As) 0.7±0.5 (Can)	3.1±2.3	0.56±0.38 (As) 0.82±0.54 (CA) 0.66±0.58 (Can)
MVK								0.7±0.3 (CA) 1.6±2.1 (Can)
Methacrolein					1.9±0.7 (TF)[m]		2.3±0.8[m]	0.48±0.22 (CA) 1.0±1.1 (Can)

[a] EMRs are relative to CO with the exception of those reported by Yuan et al. (2010). Uncertainties in literature values are the reported uncertainties or the standard deviations where multiple measurements were reported.
[b] Literature survey by Andreae and Merlet (2001) of measurements from fires in African savannas (Sv), tropical forests (TF) and extratropical forests (ET).
[c] California sage brush fires (CA) and extratropical forest fires in Montana and Colorado (ET) (Friedli et al., 2001).
[d] Savanna fires in Southern Africa (S) (Sinha et al., 2003) and prescribed fires in a savanna woodland (W) and a savanna grassland (G) (Sinha et al., 2004).
[e] Measurements reported by de Gouw et al. (2006) from aged Alaskan and Western Canada BB.

Table 3. Continued.

[f] Fires in the Mexico City region (MC) (Yokelson et al., 2007b), the Yucatan (Yu) (Yokelson et al., 2009), and tropical forest fires in Brazil (TF) (Yokelson et al., 2007a).

[g] Asian fires (As) and Canadian fires (Can) (Warneke et al., 2009).

[h] EMRs reported by Yuan et al. (2010) relative to CH_3CN from rice field crop residue fires in the Pearl River Delta, China.

[i] Mean VOC EMRs for Asian BB (As), Californian BB (CA) and Canadian BB (Can) determined using TOGA observations, unless otherwise noted. Uncertainties are the standard error in the slope of the plot of [VOC] vs. [CO] for each compound.

[j] Reported EMR is an estimate.

[k] Mean EMRs determined using CIMS HCN observations.

[l] Mean EMRs determined using PTR-MS acetaldehyde observations.

[m] Combined EMR for sum of MVK + methacrolein.

ACPD

11, 14127–14182, 2011

ARCTAS VOCs:
biomass burning
enhancements

R. S. Hornbrook et al.

Table 4. Selected literature EMRs and observed mean NMHC EMRs to CO (pptv ppbv^{-1}) by biomass burning source region during ARCTAS.

NMHC	Blake[a]	Andreae[b]	Friedli[c]	Jost[d]	Sinha[e]	Yokelson[f]	Warneke[g]	This work[i]
Ethane	8.3±0.3 (TF) 5.2±0.2 (Sv)	4.6±2.7 (Sv) 10.8±6.6 (TF) 5.2±2.2 (ET)	4.3 (CA) 6.65 (ET)	3.7	2.6±0.2 (Sv) 2.9±1.0 (W) 1.7±0.1 (G)	6.5±4.6 (MC) 9.8±5.7 (Yu) 8.7±3.7 (TF)		6.2±2.6 (As)[j] 5.8±1.3 (CA)[j] 6.0±5.0 (Can)[j]
Propane	1.6±0.1 (TF) 0.97±0.04 (Sv)	0.9±0.4 (Sv) 0.92 (TF) 1.5±0.8 (ET)	0.825 (CA) 1.88 (ET)	0.7	0.48±0.06 (Sv) 0.5±0.2 (W) 0.25±0.10 (G)	3.0±4.0 (MC) 1.5±1.3 (Yu)	3.61 (As) 0.8 (Can)	2.2±0.9 (As)[j] 1.8±0.4 (CA)[j] 3.5±5.9 (Can)[j,k]
Isobutane	0.055±0.010 (TF) 0.043±0.004 (Sv)	0.05±0.03 (Sv) 0.070 (TF) 0.10±0.05 (ET)	0.055 (CA) 0.13 (ET)	0.065	0.031±0.004 (Sv) 0.023±0.006 (W) 0.01 (G)	0.39±0.46 (MC) 0.084±0.075 (Yu)		0.34±0.19 (As) 0.08±0.04 (CA) 0.5±0.9 (Can)[k]
n-Butane	0.21±0.02 (TF) 0.16±0.01 (Sv)	0.14±0.67 (Sv) 0.19 (TF) 0.31±0.20 (ET)	0.19 (CA) 0.46 (ET)	0.19	0.087±0.007 (Sv) 0.10±0.02 (W) 0.06±0.01 (G)	1.1±1.2 (MC) 0.25±0.22 (Yu)		0.60±0.33 (As) 0.33±0.18 (CA) 0.9±1.5 (Can)[k]
Isopentane		0.07±0.07 (Sv) 0.030 (TF) 0.10±0.04 (ET)	0.035 (CA) 0.09 (ET)	0.039	0.006±0.001 (W) 0.008±0.001 (G)	0.10±0.08 (MC) 0.03±0.03 (Yu)	0.13 (As) −0.02 (Can)	0.19±0.09 (As) 0.12±0.12 (CA) 0.06±0.03 (Can)
n-Pentane	0.051±0.005 (TF) 0.053±0.005 (Sv)	0.03±0.03 (Sv) 0.052 (TF) 0.20±0.07 (ET)	0.06 (CA) 0.21 (ET)	0.062	0.017±0.005 (Sv) 0.027±0.006 (W) 0.02 (G)	0.12±0.12 (MC) 0.07±0.06 (Yu)	0.17 (As) −0.01 (Can)	0.15±0.09 (As) 0.12±0.05 (CA) 0.22±0.21 (Can)[k]
Benzene	1.29±0.05 (TF) 1.30±0.04 (Sv)	1.3±0.7 (Sv) 1.4±0.3 (TF) 1.6±0.6 (ET)	1.15 (CA) 1.35 (ET)	0.96	0.96±0.04 (Sv) 0.65±0.01 (W) 0.77±0.01 (G)	3.4±0.8 (Yu) 0.92±0.50 (TF)	1.3±0.4 (As) 1.1±0.2 (Can)	0.96±0.21 (As) 1.2±0.3 (CA) 1.4±0.4 (Can)
Toluene	0.57±0.03 (TF) 0.49±0.03 (Sv)	0.6±0.3 (Sv) 0.7±0.2 (TF) 1.2±0.5 (ET)	0.55 (CA) 1.325 (ET)	0.76	0.72±0.07 (Sv) 0.43±0.08 (W) 0.5±0.1 (G)	0.6±0.4 (TF)	0.18±0.11 (As) 0.2±0.1	0.12±0.03 (As) 0.51±0.19 (CA) 0.57±0.09 (Can)
Ethylbenzene /p-/m-xylene o-Xylene		0.24±0.13 (Sv)[h] 0.15±0.07 (TF)[h] 0.61 (ET)[h]	0.21 (CA) 0.490 (ET) 0.034 (CA) 0.11 (ET)	0.153 0.046		0.55±0.27 (TF)[h]	0.11±0.11 (As)[h] 0.12±0.10 (Can)[h]	0.09±0.06 (CA) 0.07±0.02 (Can) 0.07±0.02 (Can) 0.06±0.07 (CA) 0.06±0.02 (Can)

[a] Tropical forest fires in Brazil (TF) and savanna fires in Africa (Sv) (Blake et al., 1996).

[b] Literature survey by Andreae and Merlet (2001) of measurements from fires in African savannas (Sv), tropical forests (TF) and extratropical forests (ET).

[c] California sage brush fires (CA) and extratropical forest fires in Montana and Colorado (ET) (Friedli et al., 2001).

[d] Savanna fires in Southern Africa (Jost et al., 2003).

[e] Savanna fires in Southern Africa (S) (Sinha et al., 2003) and prescribed fires in a savanna woodland (W) and a savanna grassland (G) (Sinha et al., 2004).

[f] Fires in the Mexico City region (MC) (Yokelson et al., 2007b), the Yucatan (Yu) (Yokelson et al., 2009), and tropical forest fires in Brazil (TF) (Yokelson et al., 2007a).

[g] Asian fires (As) and Canadian fires (Can) (Warneke et al., 2009).

Title Page

Abstract | Introduction

Conclusions | References

Tables | Figures

◀◀ | ▶▶

◀ | ▶

Back | Close

Full Screen / Esc

Printer-friendly Version

Interactive Discussion

Title Page

Abstract | Introduction

Conclusions | References

Tables | Figures

◄◄ | ►►

◄ | ►

Back | Close

Full Screen / Esc

Printer-friendly Version

Interactive Discussion

Table 4. Continued.

[h] Combined EMR for sum of C_8 aromatic hydrocarbons.

[i] Mean EMRs for Asian BB (As), Californian BB (CA) and Canadian BB (Can) determined using TOGA observations, unless otherwise noted. Uncertainties are the standard error in the slope of the plot of [VOC] vs. [CO] for each compound.

[j] Mean EMRs determined using WAS observations.

[k] Excluding EMRs from Plume Group 28, the mean EMRs for Canadian BB are ethane: 4.5 ± 1.1, propane: 1.2 ± 0.4, isobutane: 0.12 ± 0.10; n-butane: 0.38 ± 0.16, n-pentane: 0.15 ± 0.05, all pptv ppbv^{-1}.
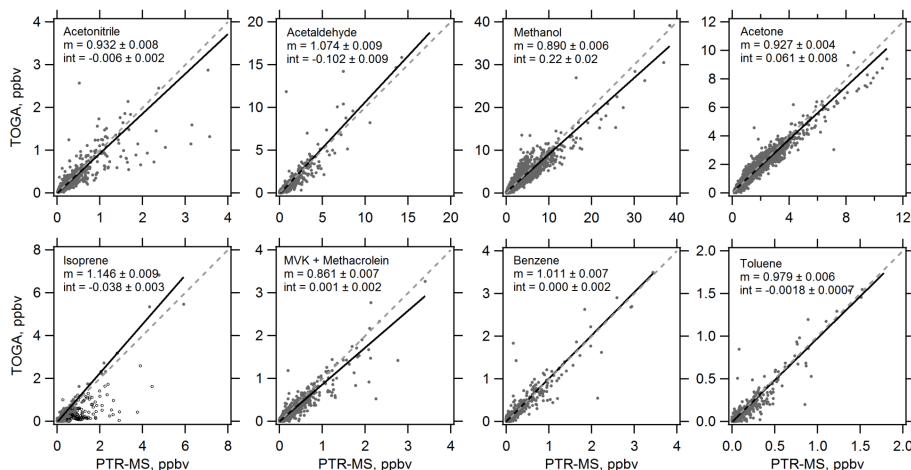
Fig. 1. Comparisons between all ARCTAS TOGA and PTR-MS observations for co-measured VOCs. Solid lines are ODR fits to the data, with slope and intercept (with 1σ standard deviations) shown on each plot. Dashed lines show $y = x$. For isoprene, only data identified as non-BB (grey points, i.e.: not listed in Table 1) are used for the ODR, as PTR-MS isoprene is reported as a sum with furan, which is present in BB. BB data are shown as black circles; using all ARCTAS isoprene data including BB data, the ODR fit has slope 0.76 ± 0.01 and intercept -0.036 ± 0.006 ppbv.
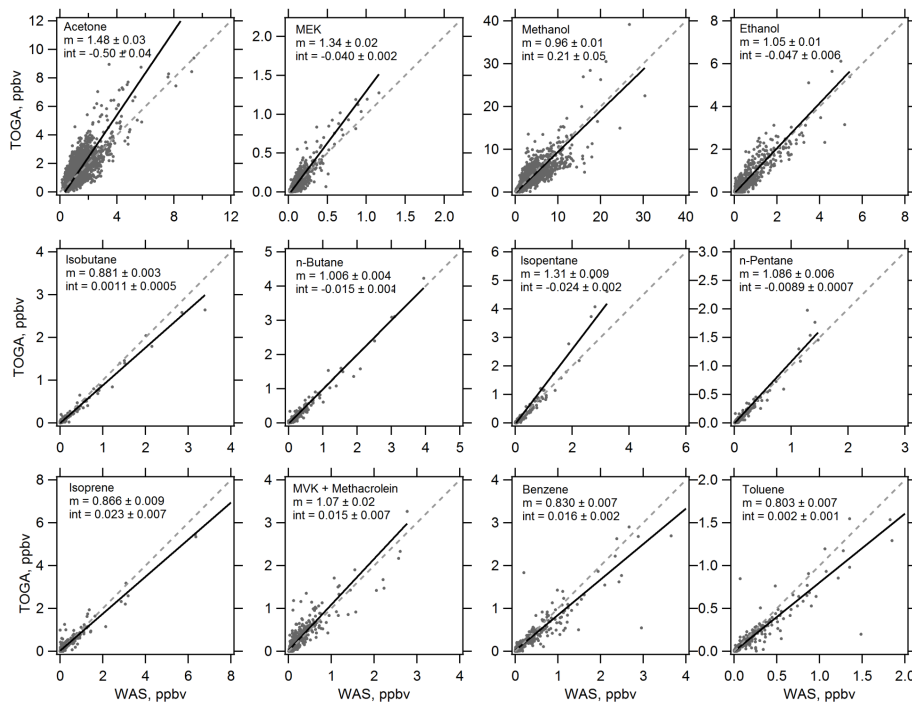
Fig. 2. Comparisons between ARCTAS TOGA and WAS observations for selected co-measured VOCs, similar to Fig. 1.

ARCTAS VOCs: biomass burning enhancements

R. S. Hornbrook et al.
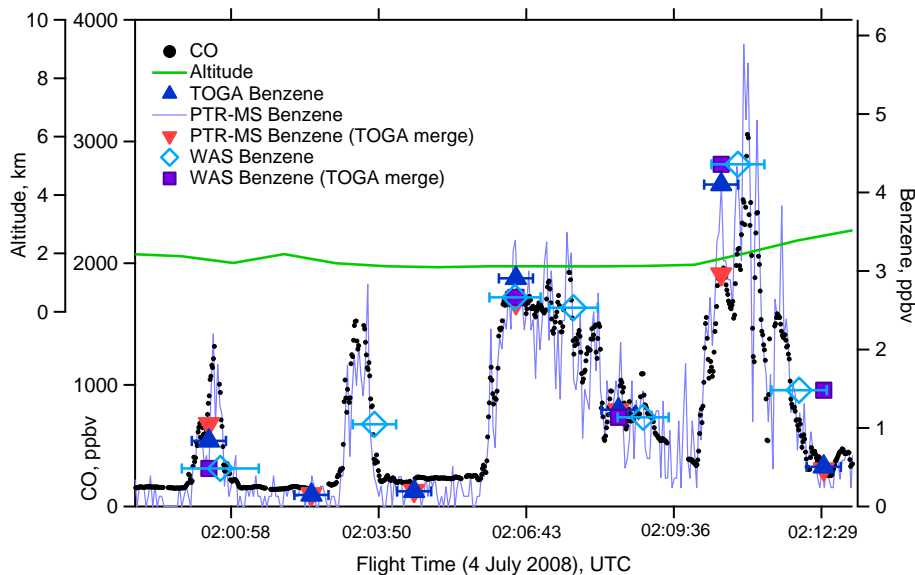
Fig. 3. Time series plot of CO, benzene observations and TOGA-merge values for benzene during a section of the 4 July 2008 ARCTAS DC-8 flight. Error bars show the start and stop times of the WAS and TOGA integrated sampling periods.
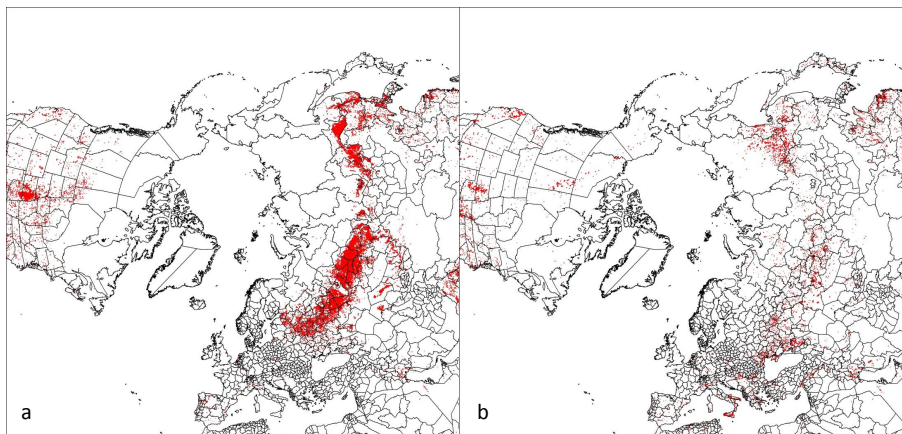
Fig. 4. Plot of the MODIS fire counts in the Northern Hemisphere during **(a)** April 2008 and **(b)** June–July 2008.
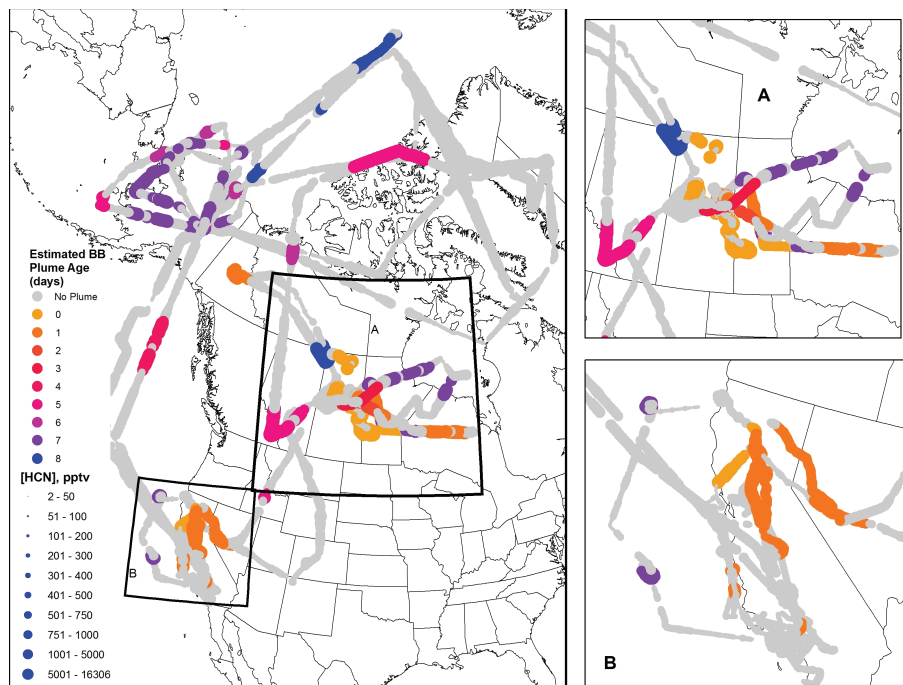
Fig. 5. Map of the plume interceptions on all the DC-8 flight paths during ARCTAS. Colored points indicate plume interceptions according to the upper legend, with estimated BB plume ages based on back trajectories, altitude, and location relative to local fires. Points are sized according to the reported HCN mixing ratio, as indicated in the lower legend. Detail map **(A)** is an expanded map showing the ARCTAS-B flights over Central Canada, and detail map **(B)** is an expanded map showing the ARCTAS-CARB flights over California.

Title Page

Abstract | Introduction

Conclusions | References

Tables | Figures

◄ | ►►

◄ | ►

Back | Close

Full Screen / Esc

Printer-friendly Version

Interactive Discussion
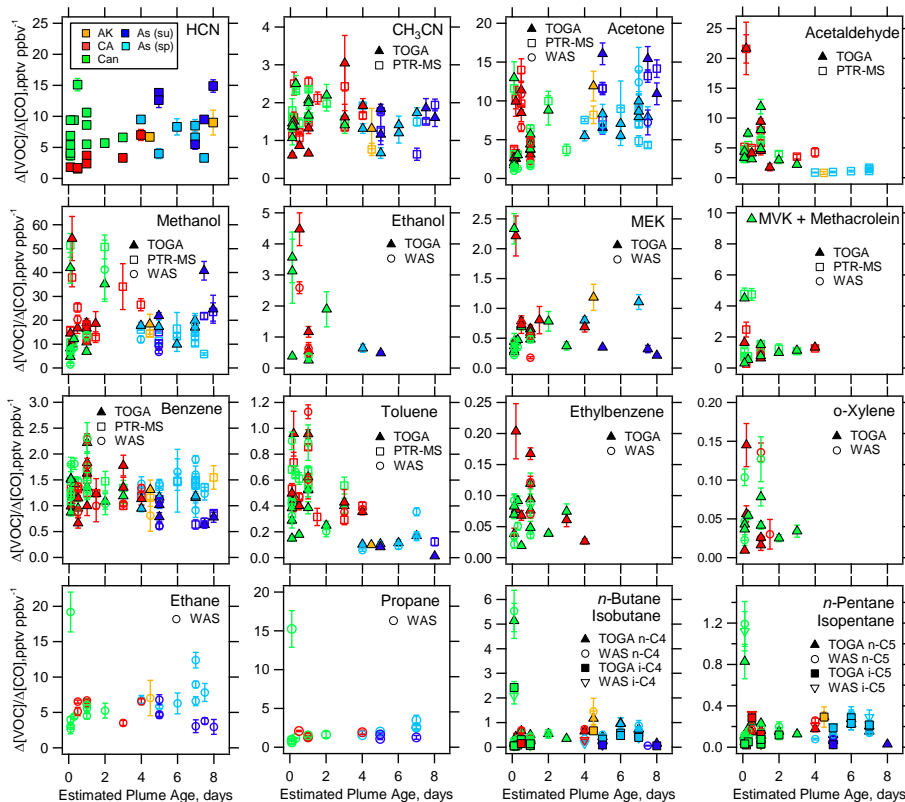
Fig. 6. Plots of observed EMRs for several VOCs to CO from individual plume groups observed during ARCTAS against estimated plume age. Error bars show the standard error in the slope of a linear fit to [VOC] vs. [CO] for each plume group. Points are colored by the BB source region and, for Asian BB, time of year (spring or summer), as shown in the legend on the HCN plot.
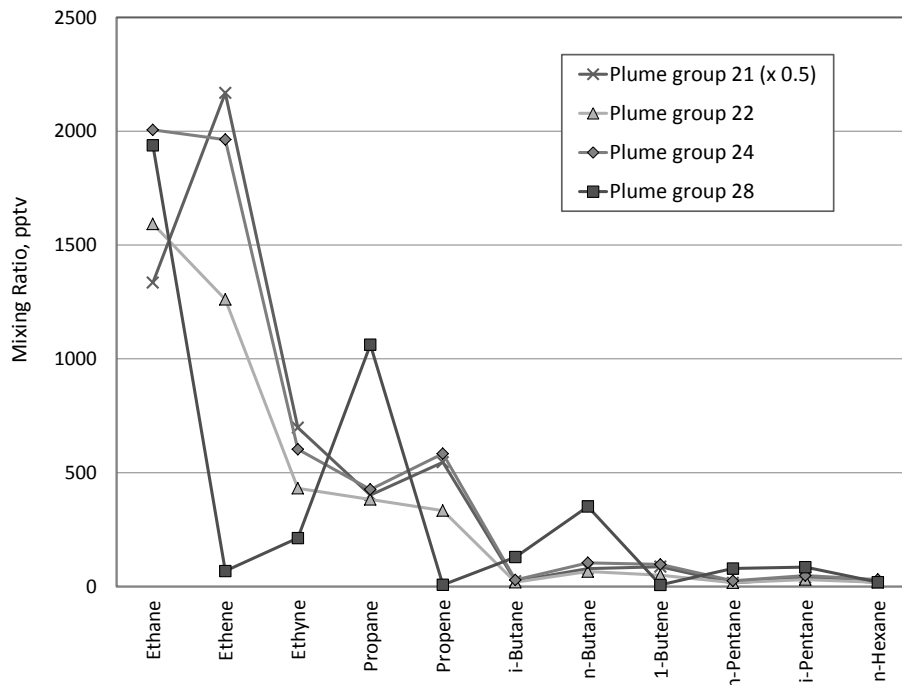
Fig. 7. Average hydrocarbon mixing ratios observed in four different Canadian BB plume groups.
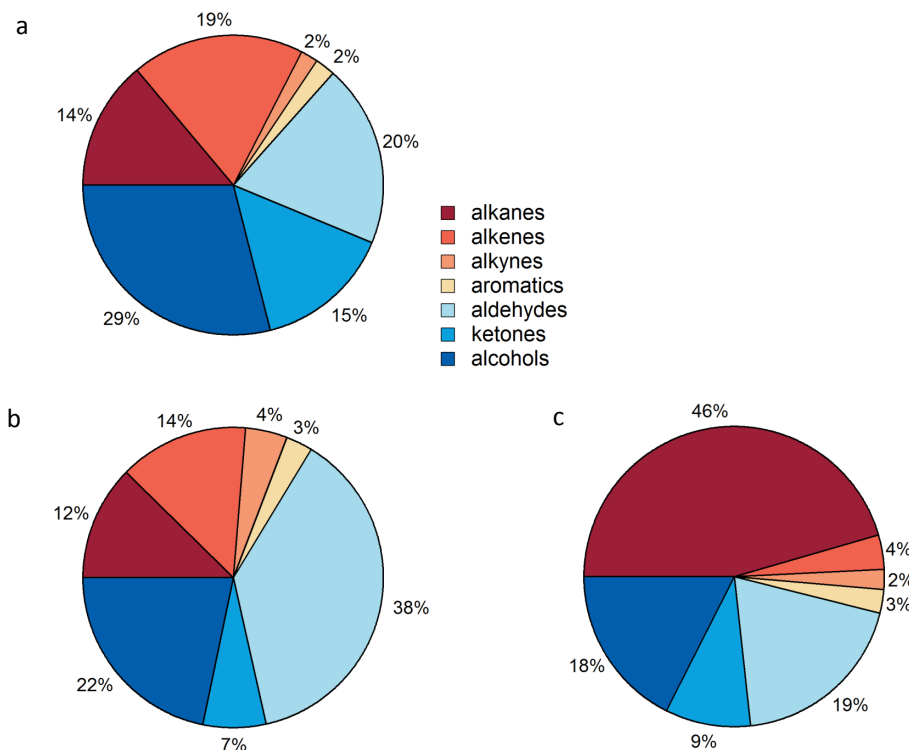
Fig. 8. VOC distributions based on the sums of mixing ratios in each compound class from selected ARCTAS observations in fresh **(a)** Canadian BB, **(b)** Californian BB and **(c)** urban emissions; **(a)** and **(b)** are the initial conditions used for the NCAR Master Mechanism box modeling.
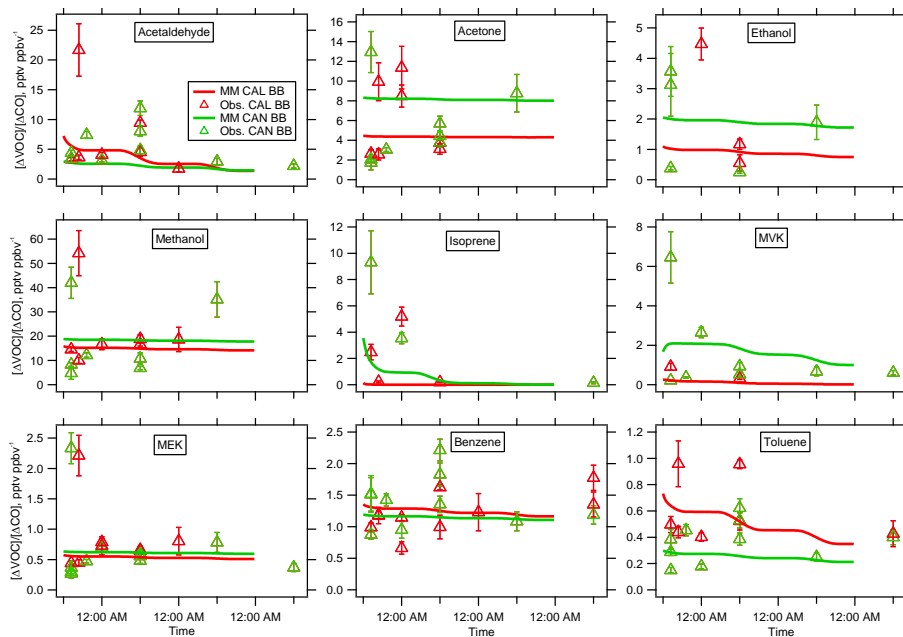
Fig. 9. Plots of modeled and observed EMRs to CO for 9 VOCs. Points are the ARCTAS TOGA-observed EMRs to CO for BB plumes estimated to be aged 3 days or less, with error bars as described for Fig. 6.
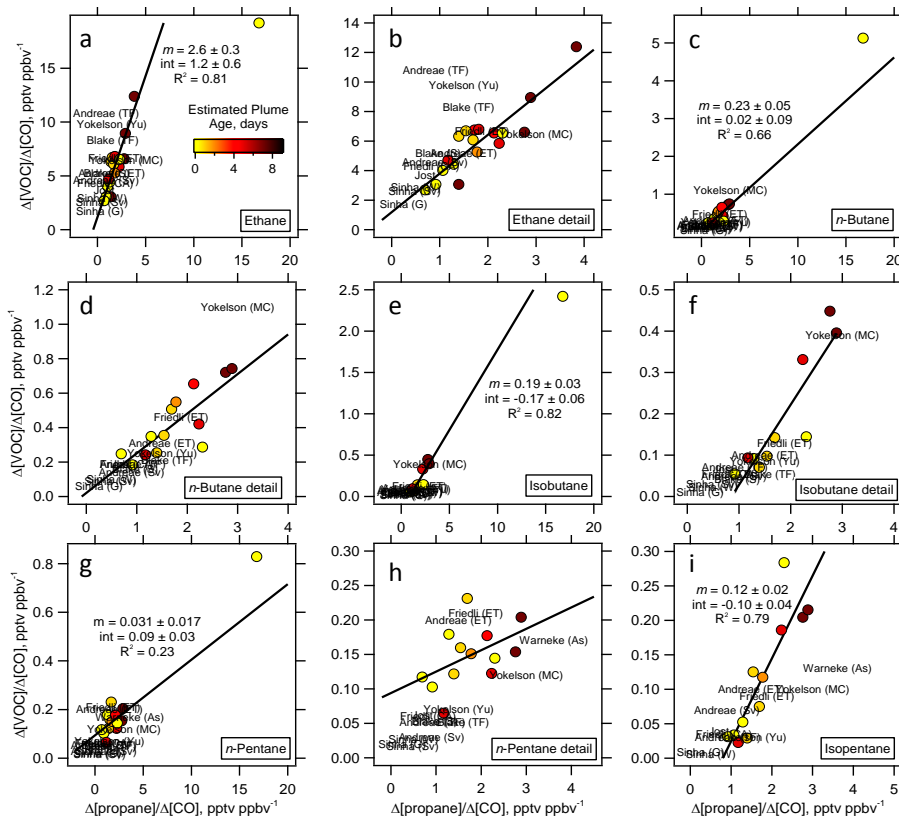
Fig. 10. Comparison plots of the EMRs to CO observed during ARCTAS for several light alkanes against propane, colored by the estimated BB plume age. Also shown are the corresponding literature EMR ratios listed in Table 4. For ethane, *n*-butane, isobutane and *n*-pentane, a second detail plot excluding the data from plume group 28 is also shown for clarity **(b, d, f, h)**. Linear least-squares fits to the ARCTAS data (excluding plume group 28 as described in the text) are shown, with details for the fits listed on each full-scale plot.

Title Page

Abstract | Introduction

Conclusions | References

Tables | Figures

|◄ | ►|

◄ | ►

Back | Close

Full Screen / Esc

Printer-friendly Version

Interactive Discussion